Prey fractionation in the Archaeocyatha and its implication for the ecology of the first animal reef systems

Running title: Prey fractionation in Archaeocyaths

Jonathan B. Antcliffe[1,2], William Jessop[1], and Allison C. Daley[1,2].

1. Oxford University Department of Zoology, South Parks Road, Oxford, UK.

2. Université de Lausanne, Institut des Sciences de la Terre, Bâtiment Géopolis, UNIL-Mouline, CH-1015 Lausanne, Switzerland.

Contacts:

Jonathan B. Antcliffe*: jonathan.antcliffe@unil.ch

William M. Jessop: will.m.jessop@gmail.com

Allison C. Daley: Allison.daley@unil.ch

* to whom correspondence should be directed.

Abstract

Archaeocyaths are the most abundant sponges from the Cambrian period, forming the first animal reef communities over 500 million years ago. The Archaeocyatha are index fossils for correlating rocks of similar ages globally, because of their abundance, extensive geographic distribution, their detailed anatomy and well established taxonomy. Their ecological significance remains incompletely explored yet they are known to strongly competitively interact unlike modern sponges. This study examines the feeding ecology of the fossil remains of Siberian archaeocyath assemblages. As suspension feeders, archaeocyaths filtered plankton from the water column through pores in their outer wall. Here we outline a new method to estimate the limit on the upper size of plankton that could be consumed by an archaeocyath during life. The archaeocyaths examined were predominantly feeding on nanoplankton and microplankton such as phytoplankton and protozooplankton. Size-frequency distributions of pore sizes from six different Siberian archaeocyath assemblages, ranging from Tommotian to Botoman in age, reveal significantly different upper limits to the prey consumed at each locality. Some of the assemblages contain specimens that could have fed on larger organisms extending in to the mesoplankton including micro-invertebrates as a possible food resource. These results show that during the establishment of the first animal reef systems, prey partitioning was established as a way of reducing competition. This method has applicability for understanding the construction and the functioning of the first reef systems, as well as helping to understanding modern reef systems and their development though time and space.

Keywords: Ecology, Sponges, Porifera, Evolution, Reef, Archaeocyatha, Cambrian, Carnivory, Prey Partitioning.

1. Introduction

The Archaeocyatha are an extinct group of aspiculate sponges (Figure 1) that appear very early in the Cambrian, forming extensive reef communities (R Core Debrenne 2007, Debrenne et al. 2012, Gandin and Debrenne 2010, Wood 1999) and shortly after the first appearance of sponge fossils (Antcliffe 2013, 2015, Antcliffe et al. 2014, Carrera and Botting 2008, Muscente et al. 2015, Nettersheim et al. 2019). While now widely recognized as an extinct class of Porifera (Antcliffe et al. 2014, Debrenne et al. 2012), their taxonomic affinities were disputed until the 1990s (Debrenne and Vacelet 1984, Kruse 1990, Rowland 2001). Given their abundance and global distribution, the archaeocyaths have become important index fossils for correlating rocks on a global scale, meaning that we have detailed knowledge of their taxonomy and systematics (Debrenne et al. 2012, Gradstein et al. 2012). The Archaeocyatha are the first undoubted metazoans to form extensive reef-like bioconstructions in association with calcimicrobes (Brasier 1976, Gandin and Debrenne 2010, Rowland and Gangloff 1988) and they therefore play a pivotal role in early Cambrian ecology (Cordie and Dornbos 2019, Wood 1999, Wood et al. 1992, Zhuravlev et al. 2015). Studies on their functional morphology have been extensive and show the Archaeocyatha were suspension feeders (Debrenne et al. 2012, Wood et al. 1992). The reef communities of archaeocyathan sponges meant many individuals lived in close proximity. Ordinarily such close assembly leads to increased competition for suspended food resources, particularly given that in the early Cambrian the global abundance of phytoplankton and zooplankton is thought to have been much lower than modern levels (Cordie et al. 2019, Servais et al. 2010). In modern animal communities, resource partitioning is a common strategy used to reduce food competition between co-existing taxa (Gili and Coma 1998). However, it has long been known that modern sponge communities do not play by the same ecological rules as most

66 metazoan communities (Reiswig 1971, Wulff 2006). Modern sponges do not partition prey before
67 ingestion, only during retention, meaning there is little competition between them for this resource
68 (Reiswig 1971). As a result sponge dominated communities are almost invariably not competition
69 driven, but neutral associations (Reiswig 1973). It seems that modern sponges are "different from
70 all the other organisms for which the conceptual framework of ecology was developed" (p. 148,
71 Wulff 2006). Sponge interactions, particularly in modern sponge dominated communities,
72 generally promote the "continued coexistence of all participating species" (p. 274, Wulff 2012).
73 Such cooperation and passive association has not been observed for many Cambrian sponge
74 communities comprised of the archaeocyaths (Zhuravlev et al. 2015). Rather, competitive
75 interactions are well documented in Archaeocyaths, including characteristics such as overgrowth
76 (bioimmuration), avoidance, and the secretion of aporous skeletal sheets to maintain barriers
77 between individuals (Brasier 1976, Debrenne et al. 2012, Kruse 1990). Statistical analysis of
78 extensive ecological datasets also indicate that archaeocyathan communities were selectively
79 assembled (Zhuravlev et al. 2015), meaning that the individuals were competing to be present in
80 the community. Archaeocyathan communities therefore behaved rather differently to modern
81 sponge dominated communities, and this seems to have been particularly true during the
82 Tommotian (Cambrian Stage 2 in Siberia, Russia),

83

84 The structure of an archaeocyath skeleton (Figure 1A and B) is thought to reflect the organization
85 of the aquiferous system in life (Wood et al. 1992). As suspension feeders, archaeocyaths filtered
86 organic matter from the water column, which they brought into their body through pores or canals
87 in their skeleton (Debrenne et al. 2012). Archaeocyaths had choanocytes (Debrenne et al. 2012)
88 that would have helped generate a current drawing water from the outside of the sponge through

the outer wall into the intervallum, the space between the inner and outer walls, and then out of the inner wall pores to where it would have exited the cup (Balsam and Vogel 1973). While some archaeocyaths were single walled (e.g. *Archaeolynthus* Figure 1C) most archaeocyaths had double walls (Figures 1A, D, E, and F), and the majority of living matter was located in the intervallum (the space between the two walls), and it would be here that phagocytosis of food would have taken place (Debrenne et al. 2012, Savarese 1992). The morphology of archaeocyaths is radically different to any living sponges, with the single genus *Vaceletia* being the only approximate morphological analogue, as the only surviving sphinctozoan sponge (Vacelet 1977, Wörheide and Reitner 1996). Sphinctozoans are a polyphyleteic grouping of similarly constructed sponges that reached their peak during the Permo-Trias (Senowbari-Daryan and García-Bellido 2002). There are many similarities between the polyphyletic sphinctozoan sponges and archaeocyaths, including the lack of spicules e.g. in *Vaceletia* (see Vacelet 1977), the massive calcareous skeleton, and the segmentation and partitioning of the skeleton (Kruse 1990). However, there are also fundamental differences such as the wall/pore elaborations in archaeocyaths, which are entirely absent in sphinctozoans. The wall microstructure is also different between archaeocyaths and sphinctozoan sponges, as is the stereoplasm, and the ontogenetic sequence of wall production, particularly in relation to the intervallum where food digestion takes place (Kruse 1990). Archaeocyaths are therefore unique in the evolutionary history of sponges, and are morphologically distinct from all living sponges.

There has been little examination of what characters of the archaeocyaths were the primary focus for the observed competitive exclusions. According to ecology theory, the primary driving factors of competition are: resources (primarily food), the natural environment (e.g. space), and natural

enemies (e.g. predators, Shea and Chesson 2002). As archaeocyaths had no known natural predators, and ecological studies suggest that they were often pioneer species so had little competition for local space (Zhuravlev et al. 2015), we here test the hypothesis that food was a limiting resource that drove competition in archaeocyathan communities. What archaeocyaths fed on is unknown, but is usually assumed to be bacteria as these are important to the diet of extant sponges (Debrenne and Zhuravlev 1997, Kruse et al. 1995). Modern sponges can feed on the whole size range of particles that can enter through their pores (ostia) albeit generally with reduced efficiency with increasing particle size (Leys and Eerkes-Medrano 2006). In archaeocyathan sponges, the size of the pores on the outer wall logically limited the size of food particles entering the skeleton, and when measured consistently, pore size can therefore provide an upper bound on the size of plankton that could have been phagocytosed by internal feeding cells. Archaeocyath outer wall pore sizes, as well as septal and inner wall pores (Figure 1A and F), have been measured as a taxonomic indicator (Kruse 1982, Kruse and Moreno-Eiris 2014, Skorlotova 2013), however, pores have never been examined in an ecological context. Here we describe the feeding dynamics and prey partitioning of archaeocyathan reef communities by using measurements of the outer wall pore diameter as a proxy for delimiting the size of suspended plankton entering the body and being consumed by the animal. Restrictive pore size data can also be used to examine the type of prey being consumed, because plankton fall broadly into distinct size categories that correlate well with biological grouping (Sieburth et al. 1978).

2. Materials

The archaeocyath material studied was derived from localities on the Siberian Platform in Russia (Figure 2A), and is housed in the collections at the Muséum National d'Histoire Naturelle (MNHN)

in Paris, France. The Siberian Platform consists of three major facies tracts of lower Cambrian, Nemakit-Daldynian to Toyonian in age, equivalent to Cambrian Series 1 (Terreneuvian) and Series 2, which displaced north-eastward throughout the Cambrian (Khomentovskiy and Repina 1965). The fossil localities are now found where the Lena and Aldan rivers intersect the archaeocyathan reef system. In general, there is a SW-NE trend of increasing palaeo-water depth (Figure 2A and B), with the archaeocyathan reef acting as a barrier between the shallow marine, evaporitic, terrigenous system to the SW and the open fully marine deeper water carbonates to the NE (Kruse et al. 1995). The specimens were predominately collected during fieldwork by Peter D. Kruse, Andrey Yu. Zhuravlev and Noel P James (Kruse et al. 1995), from six localities in Siberia: Aldan, Byd'yangaya Creek, Churan, Zhurinskiy Mys', Titirikteekh and Oy-Muran (Figure 2C). Archaeocyaths at these localities form meter-scale bioherms, where calcimicrobes, such as *Renalcis*, living in association with the archaeocyaths were responsible for precipitating the majority of the calcium carbonate that comprises the bioherms (Gandin and Debrenne 2010, James and Debrenne 1980). Taxa included in this study include the genera *Nochoroicyathus*, *Coscinocyathus*, *Rotundocyathus*, *Erismacoscinus*, and *Tumuliolynthus* (Figure 3).

The global correlations of Cambrian strata are notoriously problematic, with only a few sections in the world (mainly Gondwana e.g. Morocco and Australia, and Avalonia e.g. U.K., Canada) providing any (even if very limited) absolute dates (Landing et al. 2013). The difficulties are then compounded by major facies differences between the different global sections, leading to extreme endemism of the fossils and making global biostratigraphy problematic and contentious (Landing et al. 2013). Most stratigraphic sections contain no lower Cambrian rocks (Peters and Gaines 2012). This time period coincided with one of the largest marine transgressions in Earth history,

158 leading to subsequent extensive erosion and loss of lower Cambrian rock (Peters and Gaines 2012)
159 as sea levels receded. As a result, lower Cambrian rocks are rare and difficult to correlate. Figure
160 2D compares the locally used stratigraphic terminology for Siberia to that of the globally correlated
161 IGCP series and stages. As these correlations remain to some extent problematic (Daley et al.
162 2018, Landing et al. 2013, Rozanov et al. 2008), the internally consistent Siberian terminology is
163 adopted here, as that is how the material was catalogued in MNHN based on previous descriptions
164 and the fieldwork collection data (Kruse et al. 1995).

165

166 The Oy-Muran material is difficult to date and was collected from two areas of distinct ages within
167 the locality (Figure 2). Consequently, in the analysis they are separated according to age: one is of
168 latest Tommotian to Atdabanian (referred to as To-At Oy-Muran) and the other dated between the
169 Atdabanian and Botoman (At-Bo Oy-Muran). All the other localities are Tommotian in age.
170 Within the Tommotian, Aldan is from the oldest strata, Churan, Titirikteekh and Zhurinskiy Mys'
171 are all three derived from strata of a slightly younger age, and Byd'yangaya Creek is from the
172 youngest strata (Kruse et al. 1995). They were also separated spatially, with each locality
173 representing an area of exposed strata spaced several kilometers apart (Kruse et al. 1995) along
174 the River Lena, whilst Aldan comes from sections on the River Aldan. (Figures 2A and C).

175

176

177 **3. Methods**

178 Measurements of archaeocyaths were taken from rock thin sections mounted on glass slides. Any
179 individual archaeocyath is referred to as a specimen, such that there may be multiple specimens

on each thin section. The specimens from which measurements could be taken were identified to a genus level on each thin section by previous researchers, and when unclear they were identified with help from Dr. A. Kerner (Muséum National d'Histoire Naturelle, MNHN, Paris, France). A specimen was identified as suitable for use if it was possible to take at least five representative outer wall pore measurements, although usually around ten measurements were taken from each specimen. Pores had to be well enough preserved that the area within and around the pore could be distinguished clearly. Each thin section examined was digitally scanned and the specimens to be measured were assigned labels (Supplementary Information). A Heidenhain Quadra-Chek with a Nikon Measuring Microscope with a binocular head was used to take the measurements.

Archaeocyaths can be clonally modular, that is constructed of more than one cup (Debrenne et al. 2012) and are one of the earliest animal groups to become clonal (Landing et al. 2018). In life, the archaeocyath would have branched when creating clonal modules, which in thin section is not immediately obvious because the connection may not be visible in the plane of section. Thus, one individual might produce many cups, which could appear to be separate individuals in thin-section. This could lead to pore sizes on cups from the same individual being counted twice as separate specimens. It is therefore necessary to be able to distinguish between cups of separate individuals in close proximity and cups of one modular individual (Figure 1C, D, and E). Several indicators were used to distinguish modular forms from separate individuals, including the presence of immune responses (Brasier 1976) to dismiss the possibility of two or more morphologically similar archaeocyaths in close proximity being one modular form. Most of the archaeocyath species examined in this study were not modular as modularity was rare in the Tommotian (Wood et al. 1992).

Two different procedures were developed for measuring restrictive pore size depending on whether the section through the pore was either transverse or longitudinal (Figure 4). If a pore was cut at an angle that departed from either the longitudinal cut or the transverse cut measurements were not taken as neither technique would be appropriate (Figure 4, Figure 5A, B). This often meant entire specimens were rejected as all the pores were oblique cuts. To ensure the accuracy of the measurement from the information that can be gained from one view, each specimen was compared to different cuts of con-generic specimens. Previous studies have measured outer wall pore sizes (Kruse 1982, Kruse and Moreno-Eiris 2014, Skorlotova 2013) but do not take into account the commonly present features of pores that would have restricted the size of plankton which could pass through the pore. Such features include bracts (Figure 5C), tumuli (Figure 5D), and microporous sheaths. All of these features would have limited the size of particles that could pass into the archaeocyath. When such structures were present in the studied material, measurements were taken of the unobstructed gap left open by the additional feature. Broken walls were disregarded so as not to overestimate pore sizes (Figure 5E). When both types of view were available on the same specimen measurements were taken from both for later comparison (Figure 5F). Having both longitudinal and transverse sections provides a complementary view of the pores to gain maximum information about the shape and structure of the pore.

3.1. Measuring outer wall pore diameter in transverse view

A transverse view of an archaeocyath pore intersects the pore in a plane perpendicular to the surface of the outer wall. In thin section, pores in transverse view are visible along their entire

depth from the exterior surface to the interior surface of the outer wall (Figure 4C, right side). In some specimens, the pore is parallel-sided, alternatively the pore diameter can narrow (be funnel-shaped) along its length (Debrenne et al. 2012). In the case of a funnel-shaped pore, the restrictive pore size is the narrowest end of the pore. A transverse cut through a pore might make pore size appear smaller than it actually is if the cross-section does not cut through the pore at its maximum width (Figure 4B, top right side). Thus thin sections of archaeocyaths can be misleading (McKee 1963). To resolve this problem, measurements of restrictive pore size were only taken from the apparently largest pores on a specimen, as is the convention used by studies that measure other aspects of pore sizes (Kruse 1982, Kruse and Moreno-Eiris 2014, Skorlotova 2013). So in transverse view, restrictive pore size comes from the largest pores visible in section.

3.2. Measuring outer wall pore diameter in longitudinal view

Longitudinal views of pores intersects a pore in a plane parallel to the outer wall surface, such that the pores appear as circles in thin section. Incidentally, a longitudinal view of a pore will usually intersect the archaeocyathan cup slightly obliquely as the tangent to the cup wall, so a longitudinal cup view and a longitudinal pore view do not have to be the same, unless the wall is parallel to the cup axis. Longitudinal pore views only show the diameter of the pore at one point along its whole depth, and it can be unclear if this is the narrowest point, potentially leading to overestimation of the restrictive pore size (Figure 4C, right side). To resolve this, only the pores that appeared smallest were measured. This approach also resolved problems connected to the presence of any features associated with more complex pores. For example, if the pores had bracts it would be the gap between the bract and the pore wall (the restrictive pore size) that would appear smallest on the thin section. A few species of archaeocyaths have two distinct pore sizes, with one being

noticeably smaller than the other. On these occasions the smallest pores among the distinctly bigger pores were measured. It should be noted that specimens with two distinct pore sizes would not affect the transverse view method as the smaller pore type would be treated as an artefact and dismissed because largest visible pore diameter is measured in transverse view. Longitudinal views of pores often appeared non-circular. There are two reasons for this. Firstly, if circular pores were cut at a slightly oblique angle, then pores would appear oval shaped (McKee 1963). This is an artefact, and the true restrictive diameter can still be measured from the shortest dimension. Secondly, some archaeocyath species have true non-circular pores, although this was the case for only one taxon measured in this study. For non-circular pores, only the shortest distance was measured (the minor axis of the ellipse), as ingestion was still limited by the shortest distance across the pore.

4. Analyses

Data collected were input into Microsoft Office Excel and used to calculate mean outer wall pore sizes, standard deviation and coefficient of variance for each specimen. The statistical program R (R-Core-Team 2018) was used, specifically the packages ‘arm’ for correlation and regression analyses, and ‘ggplot2’ for plotting the figures. PAST (Hammer and Harper 2008) was used for Kolmogorov-Smirnov tests for examining data distribution. Pearson’s was used for all correlations unless otherwise stated. All results are reported as three significant figures, unless an exact result was obtained. The results are split into four parts, the first two of which aim to test the validity of the methods. The second two aim to investigate aspects of archaeocyath feeding ecology. The method of analysis for each of these categories is described below.

4.1. Analyses of transverse and longitudinal measurements from the same specimens

The aim of these tests was to determine whether the method used on longitudinal pores was measuring the same diameter as the method used to measure transverse pores. All the data for specimens across all the localities for which both longitudinal and transverse measurements had been taken were compiled, and mean pore sizes of each specimen were calculated for pores measured from the transverse and longitudinal sections separately. The two mean pore sizes were examined with linear regression, with a paired t-test performed for the support of regression gradient. The null hypothesis of these tests is that there are no significant differences between the mean pore sizes measured from transverse and longitudinal sections. Since neither the transverse or longitudinal measurements can be designated as the dependent or independent variable, two linear regressions were carried out (x on y and y on x). One was for the transverse measurement against the longitudinal measurements. This makes transverse measurements the dependent variable and so all the error is attributed to the transverse measurements. The other regression made longitudinal measurements the dependent variable so that the situation was reversed. The standard deviations and coefficient of variance of the measurements were also compared between the transverse and longitudinal datasets using t-tests and linear correlation to compare the dispersion of the measurements. The aim of these tests was to investigate whether there was equal variability in the longitudinal and transverse measurements from each individual specimen.

4.2 Analyses of transverse and longitudinal measurements when only one type of outer wall pore view was taken per specimen

Mean pore size data were collated for specimens in which pores in only one view had been measured. Although all the mean pore sizes of transverse measurements had been taken from different specimens to the longitudinal measurements, it was reasoned that for a locality the transverse and longitudinal measurements should not be significantly different from each other since the specimens for both theoretically represent a random sample of the same population. For this reason, the transverse and longitudinal measurements were only compared if they were from the same locality. The sample sizes for these tests were therefore smaller than for the previous section. Any significant differences in the overall mean of the mean pore sizes of transverse versus longitudinal measurements were tested using a Welch's t-test. A Welch's t-test was used as there would otherwise have been a slight violation in the assumption of constant variance. Data were subjected to a Box-Cox transformation to improve normality. These tests were used to investigate whether the mean pore size distribution for a locality as calculated from specimens for which only transverse measurements were taken was significantly different from the pore size distributions calculated from specimens from which only longitudinal measurement had been taken.

4.3 Comparisons of the distribution of mean outer wall pore sizes between localities

The aim of these tests was to test for any significant differences between the distribution of pore sizes found at the different localities. Comparisons were made of the distribution of pore sizes at each locality using a series of two-sample Kolmogorov-Smirnov tests, a test which does not make any assumptions about the distribution of the data. The test compares the overall distribution of two samples by comparing the maximum difference between their cumulative probability distributions (Hammer and Harper 2008). The test was carried out on every combination of

localities. As 21 tests had been carried out in total, the Benjamini-Hochberg procedure was used to control the false discovery rate, for a false discovery rate of 5%.

5. Results

5.1. Analyses of transverse and longitudinal measurements from the same specimens

5.1.1 Comparisons of the mean outer wall pore sizes

In total there were 76 specimens for which mean pore size was calculated using both transverse and longitudinal measurements. A two-tailed paired t-test between the overall mean pore sizes of the longitudinal and transverse measurements showed no significant difference ($t(75) = 0.46$, *p-value* = 0.640). This provides evidence that there is no systematic difference between the two methods. Results of the linear correlation analyses indicate that there is a highly significant correlation between the size of pores as measured by transverse and longitudinal mean pore size ($r^2 = 0.930$, $F(1,74) = 946$, *p-value* $< 2.20 \times 10^{-16}$).

An analysis of the correlation between transverse and longitudinal measurements was performed when these could be measured from the same specimen. The regression of longitudinal mean pore size on transverse mean pore size gave a slope of 0.95 and an intercept of 3.90. The regression of transverse mean pore size on longitudinal mean pore size gave a slope of 0.98 and an intercept of 0.85. The 95% confidence intervals (Table 1) for both regressions show that the intercept is not significantly different from 0 and the slope is not significantly different from 1 at the 95% confidence level, providing evidence that the two methods are measuring the same diameter. The

lower bound for the gradient of the slope is 0.96 and the upper is 1.09, which still contains a slope of 1 (Figure 6). The true relationship between the mean pore sizes as calculated by the two types of measurement would be expected to lie between these two lines with allowance to the small uncertainty of their confidence intervals. The correlation for longitudinal on transverse is excellent ($r^2 = 0.938$) and highly significant (*p-value [slope]* = 1.00×10^{-45}). The results of these tests provide good evidence that the two types of measurement are measuring the same average pore diameter.

5.1.2 Comparisons of standard deviation and coefficient of variance of measurements used to calculate mean outer wall pore size

The standard deviation was calculated for the measurements used to calculate mean pore size, there was a sample size of 70 standard deviations for transverse and longitudinal measurements. The two-tailed paired t-test gave an insignificant result (t (69) = 0.0441, p = 0.964). This indicates that the overall mean standard deviation for the transverse measurements is not significantly different from that of the longitudinal measurements. The correlation coefficient for the two variables was 0.570 (*p-value* = 1.97×10^{-7}). This highly significant correlation suggests that the standard deviation of both transverse and longitudinal measurements increase as the other increases. To test this the coefficient of variance was calculated for all the measurements for which standard deviation had been calculated. There was no correlation between the coefficient of variance for the transverse versus the longitudinal measurements (r^2 = 0.140, *p-value* = 0.235). These results support the hypothesis that the correlation in standard deviations was caused by the increase in mean pore size. Further, a paired t-test for the coefficient of variance also found no significant difference between the mean of the coefficient of variances for the two methods (t(69) = 0.345, *p-value* = 0.731). So neither method had a consistently higher coefficient of variance.

5.2. Transverse and longitudinal measurements when only one type of outer wall pore view was taken per specimen

Box plots of the data (Figure 7) show a trend of longitudinal measurements having lower medians, upper quartile and lower quartile than transverse measurements. The longitudinal measurements also have a smaller interquartile range. Statistical tests were only carried out for data from At-Bo Oy-Muran and To-At Oy- Muran since these sites had reasonably large and even sample sizes (26 for To-At Oy-Muran and 31 for At-Bo age Oy-Muran; Figure 7B). Welch's two-tailed t-tests were used on the transformed data for To-At Oy-Muran and At- Bo Oy-Muran. The result of the t-tests showed the means of the two types of measurements were significantly different from each other ($t(23.2) = 3.0491$, $p = 0.00576$ for To-At Oy-Muran and $t(28.8) = 4.00$, *p-value* = 0.000400 for At-Bo Oy-Muran). The 95% confidence intervals for the difference between the means showed that the mean longitudinal pore size was significantly less than the mean transverse pore size for both localities ($-2.22 < \mu L - \mu T < -0.42$ for To-At Oy-Muran and $-2.61 < \mu L - \mu T < -0.85$).

5.3. Summary statistics of the mean outer wall pore sizes

In total data was collected for 257 specimens. The mean pore size for all the localities data combined was 81.5µm and the median pore size was 68.8µm. The data were positively skewed so although the maximum pore size was 273 µm there were proportionally fewer high values with 75% of the data below 101µm (Figure 8). The minimum size recorded was 25.2µm.

379 *5.4. Comparisons of the distribution of mean outer wall pore sizes between localities*

380 The sample size of mean pore sizes calculated for each locality were: Aldan=14, Byd'yangaya
381 Creek=54, Churan=10, To-At Oy-Muran=32, At-Bo Oy-Muran=40, Titirikteekh=71 and
382 Zhurinskiy Mys'=35. The results for the two sample Kolmogorov-Smirnov tests are shown in the
383 Table 2. A majority of the significant results involve Aldan, suggesting that the distribution at this
384 locality is particularly distinct. Byd'yangaya Creek and To-At Oy-Muran also had significantly
385 different distributions. Aldan and Byd'yangaya Creek have a smaller mean and median pore size
386 than other localites (Table 3), and To-At Oy-muran contains relatively higher numbers of
387 specimens with large mean pore sizes. The other localities generally have distributions between
388 these extremes.

389

390 **6. Discussion of method validity**

391 *6.1. Analyses of transverse and longitudinal measurements from the same specimens*

392 The results support the hypothesis that the two methods are measuring the same pore diameter and
393 that both methods for taking measurements give a similar approximation of the mean pore size of
394 a specimen. This supports the validity of measuring a specimen's pore size with one method when
395 only one view is available. A consequence of studying fossil material from extinct organisms is
396 the difficulty of investigating any further whether the mean pore size estimated by the two methods
397 is in fact the true restrictive width. However, this uncertainty is minimized by the close agreement
398 of the two methods, which were both logically devised to measure the pore diameter at the
399 narrowest point. The methodology will allow for the rapid and reliable measurement of the
400 restrictive pore size of specimens for which only one view is available.

There are two possible causes of the variability of the measurements used to calculate the mean pore size for each specimen. One is that the variation in measurement reflects true natural variation in the pore size of a specimen. The rest of the variation would be due to measurement error, which could be caused by inaccurately measuring the diameter at the narrowest point of the pore: this is thought to have had minor effect as the equipment used was calibrated well and measured with high precision (calculated as being correct within 0.4-2μm over the measurement range of 25-273μm thereby representing an error range of 0.7%-1.6%). The other component of measurement error was the measuring of pores at a point that was not exactly the 'true' narrowest point of the pore. As explained in the Methods section this could lead to either under- or over-estimation of pore size depending on the cut of the section, this is difficult to quantify but was controlled for by examining pores from multiple orientations, as well as the comparative analysis of longitudinal and transverse cuts. The proportion of the variability attributable to these factors cannot be calculated from the data. Regardless of the cause, the results of the correlation and regression analysis suggest their impact on the study is relatively minor. Analyses suggested that standard deviation increased with mean pore size and so the overall measurement error and/or natural variability within a specimen is thought to have increased with mean pore size: either of these explanations are plausible. The effect of the increase in the variation of measurements on mean pore size calculations was reduced because the mean pore size for a specimen was based on measurements taken from multiple pores. The results showed no evidence of the variability in measurements being different for either method so the measurement error is the same for both methods. This suggests that both methods are equally reliable for measuring pore size. On this basis neither method can be recommended over the other.

6.2. Analyses of transverse and longitudinal measurements when only one type of outer wall pore view was taken per specimen

The unexpected trend for longitudinal measurements to be lower than transverse measurements in specimens with only one type of pore cross-section may be best explained by a sampling bias. Longitudinal measurements may tend to be taken from specimens with smaller pore sizes because large pores viewed in longitudinal section are more likely to appear incomplete because in this view you do not see a definite margin just a space in the wall which when very large be interpreted as dissolution or fracture of the wall. As a result, they were less suitable for inclusion in the study. This bias would explain the significant result of the t-test. Until the causes of the trend are resolved the effect it has on the data is unknown, although if the explanation suggested is correct it is likely that specimens with larger pores will be underrepresented. The effect of this should be relatively small because only 16.4% of the specimens had only longitudinal pores. If a bias is found for longitudinal measurements future studies may consider not including them. There is no evidence at the moment to suggest that these biases were present however.

The difference between the means of longitudinal and transverse pores could also reflect the measurement methods of the smallest of the minimum measures for longitudinally viewed pores and the largest of the minimum measures for transversely viewed pores. This is interesting because when the data is taken together from specimens where both pore types could be measured no significant difference could be found. This suggests that the overestimation of the mean from transverse pores alone could be being balanced out by the underestimation of the mean from the

446 longitudinal pores alone. However, it is worth noting that these measures are still based on real
447 pores and it is only the mean that is affected not the overall maximum. By performing our
448 subsequent analyses with the means of the data and not the upper range value of maximum
449 diameter for estimating prey size then we are taking a conservative approach to prey size range, as
450 a given archaeocyath by definition have had some larger pores than the mean pore size for the
451 specimen.

452

453 *6.3 Quantifying the effect of living tissue on restrictive pore size*

454 The restrictive pore size in life would have been constricted by the presence of the living cells that
455 cover the body of sponges. In the closest living modern analogue to archaeocyaths, *Vaceletia,* the
456 thickness of live cells covering the body wall is estimated to be between 2 and 20μm (Kruse 1990).
457 This comports well with direct evidence from fossil archaeocyaths which suggests that the cellular
458 layer is of a similar scale (see Figure 6 in Kruse 1990). The outer wall pore diameter is constricted,
459 therefore, by 4 to 40 μm (see Figure 9a) as the pore has living tissue around the entire
460 circumference and constricts both margins of the diameter. The effects of this constriction on the
461 present analysis is however insignificant as the error can be well constrained and becomes
462 insignificant as the pores get larger (Figure 9b). This could suggest potentially a hugely significant
463 error on the smallest of the specimens, as the minimum outer wall pores were c.25μm thus *in*
464 *extremis* the entire pore could be covered by living cells (max 40μm), rendering the pore useless
465 for suspension feeding. This implies the smallest pores had a cellular covering towards the thinner
466 range of the spectrum. The minimum cell coverage (4μm) on smallest outer wall pores measured,
467 reduces our smallest pores to c. 21μm making little difference to their likely prey. However, by
468 the time we are considering the largest pores the error is constrained between a negligible 1.45%

(for 4µm out of 273µm) to a manageable 14.5% (40µm out of 273µm). Thus when considering the maximum size of prey that could be consumed by the largest pores (273µm) measured in our study, we can constrain these pores to between 233-269µm when allowance is made for the cells covering the archaeocyath in life. These ranges are significant when one examines the size ranges of possible prey groups, as we consider below.

7. Discussion of implications for Cambrian Ecology

The data collected on outer wall pore diameters provide information on the maximum size of plankton that could enter into the intervallum to be phagocytized by the archaeocyath. This study focused on only a few sites and a few genera namely: *Nochoroicyathus*, *Coscinocyathus*, *Rotundocyathus*, *Erismacoscinus*, and *Tumuliolynthus* (Figure 3). As archaeocyaths are a diverse group with a great deal of disparity in their skeletal morphology these taxa do not represent the global range that could be found for archaeocyathan pores. It is therefore possible that the distribution of pore sizes could be different with a different sample of taxa, at different localities, and different palaeoenvironments. It is possible that other taxa could extend the range of pore sizes both upwards and downwards. Our conclusions are therefore conservative when considering total group Archaeocyatha.

How archaeocyaths fed has been the source of some debate. It has been suggested that archaeocyaths could possibly have housed symbiotic photoautotrophs that provided nutrition for the sponge (Debrenne 2007, Wood 1999). However, a photosymbiotic mode of life is now considered unlikely for a number of reasons. Firstly, many archaeocyaths, lived in areas of high

sediment input, with this high seston input, particularly of mud sized particles (Debrenne 2007, Kruse et al. 1995). As a result light penetration would have been very poor, even in the most shallow water environments that archaeocyaths inhabited, this would have made photosymbiosis unreliable and low yield. Secondly, carbon isotope data do not show the fractionations between archaeocyaths and marine cements that would be expected if the archaeocyaths were photosynthetic, this has been replicated at different sites in Australia (Surge et al. 1997), and those sites in this study from Siberia (Brasier et al. 1994). Finally, it has been argued that archaeocyaths predominantly lived in nutrient rich environments, because they are often found co-occurring with fossil organisms with shells made with the bio-limiting nutrient phosphorous as an important component (Brasier 1991, Surge et al. 1997). While such eutrophic conditions are very good for photosynthetic organisms, such as plants and free-living algae, it is very unusual to find animal-algal photosymbioses in such conditions with modern reefal associations of this type strongly correlated with nutrient poor conditions (Gili and Coma 1998, Kiessling 2009, Surge et al. 1997). As a result, it is generally thought that bacterioplankton made up the main food resource for archaeocyaths (Debrenne and Zhuravlev 1997, Kruse et al. 1995, Wood et al. 1993). This is based on comparisons to studies of modern sponge ecology that show bacteria form a substantial part of many modern sponge diets (Leys and Eerkes-Medrano 2006, Reiswig 1971) with bacterioplankton generally falling in the 0.2 to 2 μm range (see Figure 10). Outer wall pores in modern sponges are typically in the 30-60 μm range and can commonly reach 200 μm (Bergquist 1978). However, the digestion of cells takes place in the aquiferous system in specialized choanocyte chambers and the entrance to the choanocyte chambers is typically 5-10 μm (Bannister et al. 2012, Bergquist 1978), thus only particles smaller than 10 μm can be digested by most modern sponges. Particles between 10 -100 μm can enter the sponge and travel through the aquiferous system but cannot enter the

choanocyte chambers (Bannister et al. 2012). While particles over 100 μm have very little chance of entering the body of most modern sponges. The body size of archaeocyaths is significantly smaller on average than that of modern sponges (averages of 10.6mm vs 94.1mm were found according to Cordie and Dornbos 2019), yet our analysis indicates comparable outer wall pore sizes in archaeocyaths and modern sponges. However, the internal morphology of archaeocyaths is quite unlike modern sponges. In archaeocyaths digestion takes place in the intervallum between the inner and outer wall – essentially this is equivalent of the choanocyte chambers in modern sponges. The entrance to the intervallum is through the outer wall pores and there are no additional skeletal constrictions. The prey size and particle size are therefore not differentiated by the internal skeletal anatomy in archaeocyaths as they are in modern sponges. As pores in archaeocyaths are consistently two orders of magnitude larger than the size of bacteria this could make them susceptible to having to deal with higher levels of sediment input (Bell et al. 2015) which is highly problematic for sponges (Bannister et al. 2012) than would be necessary if archaeocyaths had much smaller pores. As a result, there needs to be consideration of whether larger plankton were an important part of the archaeocyath diet.

Even considering the fact that pores may have been slightly restricted by living matter, all of the archaeocyath pores measured were well over 20μm in diameter. This indicates that the whole size range of nanoplankton (2-20μm) as well as a proportion of microplankton (20-200μm) could enter the intervallum easily (Figure 10; Omori and Ikeda 1984, Sieburth et al. 1978). Generally, studies agree that phytoplankton in the nano- and microplankton size range forms a significant part of the diet in most modern sponges (see review by Riisgård and Larsen 2010). These larger plankton (nano and micro) are believed to be taken up by cells such as the amoebocytes and collenocytes

537 that line the inhalant passages (Conover 1981, Riisgård and Larsen 2010). Plankton larger than
538 5µm formed ~15% of the ingested carbon of the demosponge *Dysidea avara* but that a capacity to
539 ingest a broad range of food particles, particularly phytoplankton, was important for sustaining a
540 constant food supply during winter when nutrient flux was lower (Ribes et al. 1999). These studies
541 support the hypothesis that nanoplankton and microplankton may have formed an important part
542 of the archaeocyath diet.

543

544 Nanoplankton and microplankton size classes can be produced by an array of different organisms
545 (as can be seen from Figure 10, following (Sieburth et al. 1978)). Indeed, the 2-200µm range is
546 the only major class of plankton size that is commonly produced by a number different major types
547 of organism (e.g. the Picoplankton at 0.2-2µm size range are produced almost exclusively by
548 bacteria; the megaplankton at 20-200cm are exclusively animal). Microplankton, however, are
549 commonly produced by fungi (mycoplankton), photosynthetic eukaryotes (phytoplankton), and
550 heterotrophic eukaryotes (protozooplankton). Using the restrictive pore size data to make
551 predictions of which specific nanoplankton and microplankton were potentially being consumed
552 by these archaeocyaths is complicated by the fact that the planktonic assemblages before the Great
553 Ordovician Biodiversification are believed to have been quite different to present day assemblages
554 and very little is known about them (Servais et al. 2010). Known Cambrian phytoplankton are
555 generally classified as acritarchs (see review by Servais et al. 2010) a polyphyletic group that
556 includes any organic walled microfossil of uncertain phylogenetic affiliation (Evitt 1963), with
557 sizes on the scale of tens to low hundreds of micrometers (Butterfield 1997). This is the scale at
558 which restrictive pore sizes would start to have had an effect on which plankton could enter an
559 archaeocyath for these approximately spherical prey items. The fossilised remains of acritarchs

around the Siberian Bioherm localities (Kruse et al. 1995) suggest it is likely that these would have been available as an archaeocyath food source.

Our results also suggest that archaeocyaths were able to consume Eumetazoa. The archaeocyath restrictive pore size range in our study extends to a maximum of 273µm (max 233-269µm when considering the soft tissue range) which is well in to the range of eumetazoan zooplankton (Meta-zooplankton on Figure 10). Further, the restrictive pore size measured on the archaeocyath only needs to be the size of the smallest physical dimension of the object consumed (i.e. width), not the largest dimension (i.e. length), if the prey items are not spherical. There is substantial evidence to suggest that feeding currents cause the reorientation of non-spherical prey objects to align the smallest dimension perpendicular to the current direction allowing the consumption of much larger particles (Visser and Jonsson 2000). Metazooplankton can be as small as 50µm in length, and in particular, larval stages fall well within the microplankton size class and could uncontroversially have been consumed by an archaeocyath. Metazooplankton that act as secondary consumers, such as copepods, are commonly found at around 600µm in length (in the mesoplankton size class), and typically have a length to width ratio of around 3 to 1 (Fernandez Araoz 1991). This would mean that with a short axis size of around 200µm they could also be consumed by the larger end of the archaeocyath pore size spectrum when aligned by feeding currents. The largest pores found in our sample would allow copepods to be consumed of a size up to c.800µm in length given current alignment. This suggests that archaeocyaths could have been carnivorous similarly to many other modern sponges (Vacelet 2006, Vacelet and Boury-Esnault 1995). Most sponges that are carnivorous capture small crustaceans such as copepods (Vacelet and Boury-Esnault 1995) and do so in nutrient poor areas of the ocean where macrophagy becomes more energetically efficient

than filter feeding microscopic particles (Gili and Coma 1998). Ingesting such energetically difficult large prey items would likely necessitate a slower processing time by the archaeocyath. Studies of the ingestion of isotope tagged prey in modern sponges suggests that prey can be retained inside the sponge for a period of up to two weeks, providing considerable time-averaging of isotope fractionations with the sponge body itself (Kahn et al. 2018). It is clear that sponges can take extensive amounts of time to process food items. It is highly likely that the intervallum space in the archaeocyath (see Figure 1A) is where the ingestion of food takes place (Debrenne et al. 2012). It is possible that micro- and meso-plankton could enter this area, become trapped, and then remain there as the sponge slowly digested the item. Microscopic phosphatised fossils of 'Orsten-type' fossils provide the earliest evidence of planktonic metazoan larvae (Daley et al. 2018). These fossils are three-dimensionally replicated in phosphate and are widespread both temporally and geographically (Maas et al. 2006). Taxa such as *Yicaris dianensis* and *Wujicaris muelleri* from the phosphatic Yu'anshan Formation, China (Zhang et al. 2010, Zhang et al. 2007) are at least 514Ma old (Wolfe et al. 2016) and are directly comparable to larvae of well-studied arthropods (Zhang et al. 2010). At an age of around 514 Ma these fossils are only slightly younger than most of the archaeocyaths that comprise the present study (c.520Ma – see Figure 2), and coeval with the youngest specimens herein (Atdabanian/ Series 2 Stage 3). As a result, such prey were available to archaeocyaths.

The analysis also shows that there is significant variation in the distribution of outer wall pore sizes between some of the localities. All of the restrictive pore sizes were within the microplankton range, but some archaeocyathan assemblages had significantly larger restrictive pores sizes, and thus could have consumed larger microplankton. Specimens from Aldan and Byd'yangaya have

606 significantly smaller restrictive pore sizes than the other localities, meaning the archaeocyaths had
607 a narrower range of possible prey items and a smaller upper limit on prey size. The specimens
608 measured from To-At Oy-Muran had significantly larger restrictive pore sizes and so would have
609 had the potential to take up a greater proportion of larger microplankton and potentially even the
610 mesoplankton.

611

612 Regional variations in fossil compositions are commonly attributed to a combination of ecological,
613 environmental and taphonomic factors (Zhao et al. 2012). Taphonomic explanations probably have
614 a limited role in causing pore size variation, because archaeocyath pores are usually well preserved.
615 Outer wall pore size variation is more likely the result of differing compositions of planktonic
616 communities at different localities, with archaeocyaths at each having adapted to extract the range
617 of plankton sizes that are found in higher abundance. It could also be that species with larger pores
618 could potentially have fed on a wider variety of plankton, lending flexibility to their feeding mode,
619 which would be advantageous in many situations, for instance during seasonal variations in food
620 abundance. In bioherms where there was more intense competition for the food resource, variations
621 in pore sizes could allow resource partitioning in the archaeocyaths. Other factors could alter local
622 archaeocyathan community composition; not least of which are their many other morphological
623 characters that are also subject to selection. The present study shows that outer wall pore size
624 differences are statistically significant between sites, and that this is therefore one character worthy
625 of consideration when exploring ecological and evolutionary scenarios, but it does not preclude
626 other factors also being significant.

627

628 Prey partitioning allows many species to form a single assemblage in a given location without
629 increasing competition to unsustainable levels whereby the assemblage would disintegrate. Thus
630 in one hydrodynamic regime a high diversity system can be established and maintained (Lesser et
631 al. 1994). This is most readily achieved by limiting the range of prey size choice. Organisms that
632 ingest small particles and require higher flow rates can then live in the same place as organisms
633 that ingest larger particles and can therefore tolerate much lower flow rates (but will happily live
634 in areas of high flow rate (Gili and Coma 1998)). Active suspension feeders that generate currents
635 to bring prey towards themselves are more energetically efficient at eating small prey, and sponges
636 are remarkably efficient at this, expending only 0.8% of respiratory energy on pumping (Riisgaard
637 and Larsen 1995). So changes in prey size, though effecting this efficiency, are not critical to the
638 ability to survive in a particular hydrodynamic regime, as the filtration system in sponges is so
639 energetically efficient. In modern oceans, sponges dominate deep sea filtration but cnidarian reefs
640 dominate in shallow temperate seas (Gili and Coma 1998). This is not the case in the Cambrian
641 when there were no coral dominant reefs (not until the Tabulate coral reefs of the Ordovician, see
642 Landing et al. 2018), and when archaeocyathan reefs dominated the shallow marine successions
643 in epicontinental seas from temperate to tropical waters (Gandin and Debrenne 2010). It is
644 therefore quite possible that archaeocyaths functioned more like modern coral reefs than like
645 modern sponge reefs. In this sense, they would have dominated the energy flow from the pelagic
646 to benthic system in Cambrian seas.

647

648 The variation in the average upper bound of the size of plankton archaeocyaths could take up could
649 also be influenced by other factors. For example, bracts (see Figure 5C), which reduce the size of
650 food particle that could enter the archaeocyath, are proposed to be an adaptation to environmental

651 factors such as locally high water turbulence (Debrenne et al. 2012). This could mean that variation
652 in pore size distributions reflects variation in water turbulence between the localities. Water
653 turbulence, flow rate, and seston concentration are all crucial factors that affect how efficiently
654 filter feeders can take up prey (Gili and Coma 1998), however they are all connected to prey
655 selection and are themselves not mutually exclusive factors. Bioherms at the Siberian localities are
656 split into domains, each of which would have had a different microclimate (Kruse et al. 1995). The
657 fossil sites examined can be divided in to two main groups based on field observations (of, Gandin
658 and Debrenne 2010, Kruse et al. 1995, Rozanov et al. 2008). The first of these is a lower diversity
659 and lower energy grouping of Aldan + Byd'yangaya + Churan which are characterized by high
660 proportions of the encrusting calcimicrobe *Renalcis* (James and Gravestock 1990), lower levels of
661 mud input, and containing small archaeocyaths which are mainly of the stick and bowl type. The
662 second type is a higher diversity and higher energy grouping of Oy Muran + Titirikteekh +
663 Zhurinskiy Mys'which are characterized by lower proportion of *Renalcis*, high levels of mud input,
664 and by a full array of archaeocyath types including large stick archaeocyaths and large ramose
665 archaeocyaths as well as the smaller types found elsewhere (Kruse et al. 1995). This fits well with
666 the data from the pairwise mean pore sizes between sites, which found that Aldan and Byd'yangaya
667 and Churan were statistically similar but that Aldan was significantly different from all the other
668 sites, whilst high levels of support were also found for distinguishing Byd'yangaya from the
669 Tommotian Oy Muran. The highly erect and ramose forms found at Oy-Muran, Titirikteekh, and
670 Zhurinskiy Mys' alongside a much higher diversity suggests these sites had much higher water
671 flow rates and higher seston concentrations, which sustained the more complex forms and thereby
672 allowed the development of much greater taxon heterogeneity. This suggest that at these three
673 higher energy sites, the sponge/*Renalcis* reef was functioning much more like a modern highly

674 heterogeneous community (such a tropic coral-algal system) than a low diversity system such as a
675 deep water sponge community. These reefs, particularly those found on the transition zone
676 between shallow and deep water (Gili and Coma 1998), as is the case for the Siberian
677 archaeocyathan reef (Kruse et al. 1995, Rozanov et al. 2008), are maintained by extensive prey
678 partitioning. This takes place across a broad range of prey sizes from picoplankton to
679 mesoplankton with prey ranging from bacteria to metazoan plankton. These highly structured
680 communities are also associated with highly structured and diverse plankton and this was likely
681 the case for the Siberian reefs of the lower Cambrian. This indicates that the planktonic system
682 was well developed by the Tommotian stage (c.525-521Ma ago) with ecosystem construction well
683 underway by this time. Archaeocyathan reefs were a critical locus for sustaining and expanding
684 biodiversity just like modern coral barrier reefs. The central and essential role that archaeocyathan
685 reefs must have therefore played in the Cambrian explosion and the accelerating metazoan
686 ecological expansion can hardly be overstated.

687

688 **8. Conclusions**

689 This study has developed, tested, and applied a new methodology for investigating the feeding
690 ecology of archaeocyaths. By following the specific methods recommended here, restrictive outer
691 wall pore size data can be measured quickly and easily from pores preserved in both transverse
692 and longitudinal section. Archaeocyath skeletons are regularly preserved with their pores intact
693 and our method provides a novel means of gathering ecologically useful information from these
694 extinct sponges. Statistical analyses of restrictive pore size data identified differences between
695 Siberian localities, and implicates prey partitioning as a likely cause. The study also provides
696 evidence that nanoplankton, microplankton, and mesoplankton could have made up some

proportion of the archaeocyath diet, in contrast to previous assumptions that they were bacteriophages. As sponges provide a critical link in marine ecosystems connecting the energy contained in the plankton to the benthos (Gili and Coma 1998), it is essential to understand the role archaeocyaths played in the early Cambrian oceans. As the first metazoan-dominated ecosystems were constructed during the Cambrian Explosion, the roles of prey partitioning and intraspecific competition can now be understood during the construction of the first complex reef ecosystems. Further, while the Archaeocyatha are confined to the Cambrian Period they are not the only group of sponges to have adopted such a peculiar mode of construction (Antcliffe et al. 2014, Debrenne et al. 2012, Senowbari-Daryan and García-Bellido 2002). This raises the prospect that other sponges that possessed large chambers and large pores (often over 1mm), and could have, therefore, ingested zooplankton and may be more ecologically complex. These sphinctozoan forms are hugely abundant and diverse, reaching an acme in the Permo-Trias before becoming almost extinct at the end Cretaceous extinction (Senowbari-Daryan and García-Bellido 2002). While they have meaningful morphological differences in comparison to archaeocyaths they could still be prey fractionating using their pores. This methodology could therefore be of broad applicability to understanding the sponge contribution to reef dynamics through much of the Phanerozoic.

9. Availability of data and support materials.

Supplementary data is hosted online associated with this publication.

10. Funding

719 WJ acknowledges funding from Jesus College (Oxford University), an Allison R. “Pete” Palmer
720 Award from the Palaeontological Society, and the Palaeontological Association (grant reference:
721 PA-UB201502). ACD and JBA acknowledge funding from the Oxford University Museum of
722 Natural History and the support of the University of Lausanne, Switzerland.

723

724 **11. Authors’ contributions**

725 JBA and ACD designed the research. WJ collected data in the collection of the MNHN (Paris,
726 France) and performed initial statistics under guidance of JBA and ACD. JBA performed further
727 statistical tests and reran all statistics for robustness. WJ photographed specimens. JBA made all
728 the figures and plates. WJ helped to draft the manuscript. JBA was the primary manuscript writer.
729 JBA and ACD developed and wrote the discussion and conclusion.

730

731 **12. Acknowledgements**

732 The authors would like to thank Graham Taylor (Zoology, Oxford) and Peter Kruse (South
733 Australia Museum) for their advice and helpful discussions. Adeline Kerner (MNHN, Paris)
734 organized access to the fossils and helped to identify specimens. Françoise Debrenne (MNHN,
735 Paris) is thanked for her extraordinary contribution to this field and for her help and encouragement
736 over many years.

737

738 **13. REFERENCES**

739 Antcliffe, J. B. 2013. Questioning the evidence of organic compounds called sponge biomarkers.
740 Palaeontology 56(5):917-925.
741 Antcliffe, J. B. 2015. The oldest compelling evidence for sponges is still early Cambrian in age–reply to Love
742 and Summons (2015). Palaeontology 58(6):1137-1139.
743 Antcliffe, J. B., R. H. Callow, and M. D. Brasier. 2014. Giving the early fossil record of sponges a squeeze.
744 Biological Reviews 89(4):972-1004.

745 Balsam, W. L., and S. Vogel. 1973. Water movement in archaeocyathids: evidence and implications of
746 passive flow in models. Journal of Paleontology 47(5):979-984.
747 Bannister, R., C. Battershill, and R. De Nys. 2012. Suspended sediment grain size and mineralogy across
748 the continental shelf of the Great Barrier Reef: Impacts on the physiology of a coral reef sponge.
749 Continental Shelf Research 32:86-95.
750 Bell, J. J., E. McGrath, A. Biggerstaff, T. Bates, H. Bennett, J. Marlow, and M. Shaffer. 2015. Sediment
751 impacts on marine sponges. Marine pollution bulletin 94(1-2):5-13.
752 Bergquist, P. R. 1978. Sponges. University of California Press.
753 Brasier, M. 1976. Early Cambrian intergrowths of archaeocyathids, *Renalcis*, and pseudostromatolites
754 from South Australia. Palaeontology 19(2):223-245.
755 Brasier, M. 1991. Nutrient flux and the evolutionary explosion across the Precambrian-Cambrian
756 boundary interval. Historical Biology 5(2-4):85-93.
757 Brasier, M. D., R. M. Corfield, L. A. Derry, A. Y. Rozanov, and A. Y. Zhuravlev. 1994. Multiple Delta-13c
758 Excursions Spanning the Cambrian Explosion to the Botomian Crisis in Siberia. Geology 22(5):455-
759 458.
760 Butterfield, N. J. 1997. Plankton ecology and the Proterozoic-Phanerozoic transition. Paleobiology
761 23(2):247-262.
762 Carrera, M. G., and J. P. Botting. 2008. Evolutionary history of Cambrian spiculate sponges: implications
763 for the Cambrian evolutionary fauna. Palaios 23(3):124-138.
764 Conover, R. J. 1981. Nutritional strategies for feeding on small suspended particles. Pp. 363-395. *In* A. R.
765 Longhurst, ed. Analysis of marine ecosystems.
766 Cordie, D. R., and S. Q. Dornbos. 2019. Restricted morphospace occupancy of early Cambrian reef-building
767 archaeocyaths. Paleobiology:1-16.
768 Cordie, D. R., S. Q. Dornbos, P. J. Marenco, T. Oji, and S. Gonchigdorj. 2019. Depauperate skeletonized
769 reef-dwelling fauna of the early Cambrian: Insights from archaeocyathan reef ecosystems of
770 western Mongolia. Palaeogeography, Palaeoclimatology, Palaeoecology 514:206-221.
771 Daley, A. C., J. B. Antcliffe, H. B. Drage, and S. Pates. 2018. Early fossil record of Euarthropoda and the
772 Cambrian Explosion. Proceedings of the National Academy of Sciences 115(21):5323-5331.
773 Debrenne, F. 2007. Lower Cambrian archaeocyathan bioconstructions. Comptes Rendus Palevol 6(1-2):5-
774 19.
775 Debrenne, F., and J. Vacelet. 1984. Archaeocyatha: Is the sponge model consistent with their structural
776 organisation? Palaeontographica Americana 54:358–369.
777 Debrenne, F., and A. Y. Zhuravlev. 1997. Cambrian food web: A brief review. Geobios 30:181-188.
778 Debrenne, F., A. Y. Zhuravlev, and P. D. Kruse. 2012. Part E, Revised, Volume 4, General features of the
779 Archaeocyatha. Pp. 1-102. Treatise Online. University of Kansas.
780 Debrenne, F., A. Y. Zhuravlev, and A. Y. Rozanov. 1989. Pravil'nye arkheot□s□iaty [Regular
781 archaeocyaths]. Trudy Paleontologicheskiy Institut Akademiya Nauk Moscow.
782 Evitt, W. R. 1963. A discussion and proposals concerning fossil dinoflagellates, hystrichospheres, and
783 acritarchs, II. Proceedings of the National Academy of Sciences 49(3):298-302.
784 Fernandez Araoz, N. C. 1991. Individual biomass, based on body measures, of copepod species considered
785 as main forage items for fishes of the Argentine shelf. Oceanologica Acta 14(6):575-580.
786 Gandin, A., and F. Debrenne. 2010. Distribution of the archaeocyath-calcimicrobial bioconstructions on
787 the Early Cambrian shelves. Palaeoworld 19(3-4):222-241.
788 Gili, J.-M., and R. Coma. 1998. Benthic suspension feeders: their paramount role in littoral marine food
789 webs. Trends in Ecology & Evolution 13(8):316-321.
790 Gradstein, F. M., J. G. Ogg, M. Schmitz, and G. Ogg. 2012. The geologic time scale 2012. elsevier,
791 Amsterdam.
792 Hammer, Ø., and D. A. Harper. 2008. Paleontological data analysis. John Wiley & Sons.

James, N. P., and F. Debrenne. 1980. Lower Cambrian bioherms: Pioneer reefs of the Phanerozoic. Acta Palaeontologica Polonica 25(3-4).

James, N. P., and D. I. Gravestock. 1990. Lower Cambrian shelf and shelf margin buildups, Flinders Ranges, South Australia 1. Sedimentology 37(3):455-480.

Kahn, A. S., J. W. Chu, and S. P. Leys. 2018. Trophic ecology of glass sponge reefs in the Strait of Georgia, British Columbia. Scientific Reports 8(1):756.

Khomentovskiy, V., and L. Repina. 1965. The Lower Cambrian of the stratotype section of Siberia. Akademia Nauk SSSR Sibirskoe Otdelenie, Institut Geologii i Geofiziki 14.

Kiessling, W. 2009. Geologic and biologic controls on the evolution of reefs. Annual Review of Ecology, Evolution, and Systematics 40:173-192.

Kruse, P. D. 1982. Archaeocyathan biostratigraphy of the Gnalta Group at Mt. Wright, New South Wales. Palaeontographica Abteilung A 177:129-212.

Kruse, P. D. 1990. Are archaeocyaths sponges, or are sponges archaeocyaths. Pp. 310-323. The Evolution of a late Precambrian-early Palaeozoic rift complex: the Adelaide Geosyncline. Geological Society of Australia, Special Publication 16

Kruse, P. D., and E. Moreno-Eiris. 2014. Archaeocyaths of the White Point Conglomerate, Kangaroo Island, South Australia. Alcheringa 38(1):1-64.

Kruse, P. D., A. Y. Zhuravlev, and N. P. James. 1995. Primordial metazoan-calcimicrobial reefs: Tommotian (early Cambrian) of the Siberian platform. Palaios 10:291-321.

Landing, E., J. B. Antcliffe, G. Geyer, A. Kouchinsky, S. S. Bowser, and A. Andreas. 2018. Early evolution of colonial animals (Ediacaran Evolutionary Radiation–Cambrian Evolutionary Radiation–Great Ordovician Biodiversification Interval). Earth Science Reviews 178:105-135.

Landing, E., G. Geyer, M. D. Brasier, and S. A. Bowring. 2013. Cambrian Evolutionary Radiation: Context, correlation, and chronostratigraphy-Overcoming deficiencies of the first appearance datum (FAD) concept. Earth-Science Reviews 123:133-172.

Lesser, M. P., J. D. Witman, and K. Sebnens. 1994. Effects of flow and seston availability on scope for growth of benthic suspension-feeding invertebrates from the Gulf of Maine. The Biological Bulletin 187(3):319-335.

Leys, S. P., and D. I. Eerkes-Medrano. 2006. Feeding in a calcareous sponge: particle uptake by pseudopodia. The Biological Bulletin 211(2):157-171.

Maas, A., A. Braun, X.-P. Dong, P. C. Donoghue, K. J. Müller, E. Olempska, J. E. Repetski, D. J. Siveter, M. Stein, and D. Waloszek. 2006. The 'Orsten'—more than a Cambrian Konservat-Lagerstätte yielding exceptional preservation. Palaeoworld 15(3-4):266-282.

McKee, E. H. 1963. Ontogenetic stages of the archaeocyathid *Ethmophyllum whitneyi* Meek. Journal of Paleontology 37:287-293.

Muscente, A., F. M. Michel, J. G. Dale, and S. Xiao. 2015. Assessing the veracity of Precambrian 'sponge' fossils using *in situ* nanoscale analytical techniques. Precambrian Research 263:142-156.

Nettersheim, B. J., J. J. Brocks, A. Schwelm, J. M. Hope, F. Not, M. Lomas, C. Schmidt, R. Schiebel, E. C. M. Nowack, P. De Deckker, J. Pawlowski, S. S. Bowser, I. Bobrovskiy, K. Zonneveld, M. Kucera, M. Stuhr, and C. Hallmann. 2019. Putative sponge biomarkers in unicellular Rhizaria question an early rise of animals. Nature Ecology & Evolution.

Omori, M., and T. Ikeda. 1984. Methods in marine zooplankton ecology John Wiley and Sons, New York.

Peters, S. E., and R. R. Gaines. 2012. Formation of the 'Great Unconformity'as a trigger for the Cambrian explosion. Nature 484(7394):363.

R-Core-Team. 2018. R: A language and environment for statistical computing. R Foundation for statistical computing Vienna, Austria https://www.R-project.org/.

Reiswig, H. 1973. Population dynamics of three Jamaican Demospongiae. Bulletin of Marine Science 23(2):191-226.

Reiswig, H. M. 1971. Particle feeding in natural populations of three marine demosponges. The Biological Bulletin 141(3):568-591.

Ribes, M., R. Coma, and J.-M. Gili. 1999. Natural diet and grazing rate of the temperate sponge *Dysidea avara* (Demospongiae, Dendroceratida) throughout an annual cycle. Marine Ecology Progress Series 176:179-190.

Riisgaard, H. U., and P. S. Larsen. 1995. Filter-feeding in marine macro-invertebrates: Pump characteristics, modelling and energy cost. Biological Reviews 70(1):67-106.

Riisgård, H. U., and P. S. Larsen. 2010. Particle capture mechanisms in suspension-feeding invertebrates. Marine Ecology Progress Series 418:255-293.

Rowland, S. M. 2001. Archaeocyaths—a history of phylogenetic interpretation. Journal of Paleontology 75(6):1065-1078.

Rowland, S. M., and R. A. Gangloff. 1988. Structure and paleoecology of Lower Cambrian reefs. Palaios 3:111-135.

Rozanov, A. Y., V. Khomentovskiy, Y. Y. Shabanov, G. Karlova, A. Varlamov, V. Luchinina, Y. E. Demidenko, P. Y. Parkhaev, I. Korovnikov, and N. Skorlotova. 2008. To the problem of stage subdivision of the Lower Cambrian. Stratigraphy and Geological Correlation 16(1):1-19.

Savarese, M. 1992. Functional analysis of archaeocyathan skeletal morphology and its paleobiological implications. Paleobiology 18(4):464-480.

Senowbari-Daryan, B., and D. C. García-Bellido. 2002. Fossil 'Sphinctozoa': chambered sponges (polyphyletic). Pp. 1511-1538. *In* J. N. A. Hooper, R. W. M. Van Soest, and P. Willenz, eds. Systema porifera. Springer, Boston, U.S.A. .

Servais, T., A. W. Owen, D. A. Harper, B. Kröger, and A. Munnecke. 2010. The great ordovician biodiversification event (GOBE): the palaeoecological dimension. Palaeogeography, Palaeoclimatology, Palaeoecology 294:99-119.

Shea, K., and P. Chesson. 2002. Community ecology theory as a framework for biological invasions. Trends in Ecology and Evolution 17(4):170-176.

Sieburth, J. M., V. Smetacek, and J. Lenz. 1978. Pelagic ecosystem structure: Heterotrophic compartments of the plankton and their relationship to plankton size fractions 1. Limnology and Oceanography 23(6):1256-1263.

Skorlotova, N. A. 2013. New archaeocyatha from the Atdabanian Stage of the Siberian Platform. Paleontologicheskiy Zhurnal 47(6):555-561.

Surge, D. M., M. Savarese, J. Robert Dodd, and K. C. Lohmann. 1997. Carbon isotopic evidence for photosynthesis in Early Cambrian oceans. Geology 25(6):503-506.

Vacelet, J. 1977. Une nouvelle relique du Secondaire: un représentant actuel des éponges fossiles Sphinctozoaires. Comptes rendus de l'Académie des Sciences 285:509-511.

Vacelet, J. 2006. New carnivorous sponges (Porifera, Poecilosclerida) collected from manned submersibles in the deep Pacific. Zoological Journal of the Linnean Society 148(4):553-584.

Vacelet, J., and N. Boury-Esnault. 1995. Carnivorous sponges. Nature 373(6512):333-335.

Visser, A. W., and P. R. Jonsson. 2000. On the reorientation of non-spherical prey particles in a feeding current. Journal of plankton research 22(4):761-777.

Wolfe, J. M., A. C. Daley, D. A. Legg, and G. D. Edgecombe. 2016. Fossil calibrations for the arthropod Tree of Life. Earth-Science Reviews 160:43-110.

Wood, R. 1999. Reef evolution. Oxford University Press.

Wood, R., A. Y. Zhuravlev, and A. Chimed-Tseren. 1993. The ecology of Lower Cambrian buildups from Zuune Arts, Mongolia: implications for early metazoan reef evolution. Sedimentology 40(5):829-858.

Wood, R., A. Y. Zhuravlev, and F. Debrenne. 1992. Functional biology and ecology of Archaeocyatha. Palaios 7:131-156.

Wörheide, G., and J. Reitner. 1996. "Living fossil" sphinctozoan coralline sponge colonies in shallow water caves of the Osprey Reef (Coral Sea) and the Astrolabe Reefs (Fiji Islands). Pp. 145-148. *In* J. Reitner, F. Neuweiler, and F. Gunkel, eds. Global and regional controls on biogenic sedimentation: 1 Reef evolution, Research Reports. Geologisch-Paläontologisches Institut der Georg-August-Universität, Göttingen, Germany.

Wulff, J. 2012. Ecological interactions and the distribution, abundance, and diversity of sponges. Pp. 273-344. Advances in Marine Biology. Elsevier.

Wulff, J. L. 2006. Ecological interactions of marine sponges. Canadian Journal of Zoology 84(2):146-166.

Zhang, X.-g., A. Maas, J. T. Haug, D. J. Siveter, and D. Waloszek. 2010. A eucrustacean metanauplius from the Lower Cambrian. Current Biology 20(12):1075-1079.

Zhang, X.-g., D. J. Siveter, D. Waloszek, and A. Maas. 2007. An epipodite-bearing crown-group crustacean from the Lower Cambrian. Nature 449(7162):595.

Zhao, F., S. Hu, J.-B. Caron, M. Zhu, Z. Yin, and M. Lu. 2012. Spatial variation in the diversity and composition of the Lower Cambrian (Series 2, Stage 3) Chengjiang biota, Southwest China. Palaeogeography, Palaeoclimatology, Palaeoecology 346:54-65.

Zhuravlev, A. Y., E. B. Naimark, and R. A. Wood. 2015. Controls on the diversity and structure of earliest metazoan communities: early Cambrian reefs from Siberia. Earth Science Reviews 147:18-29.

Table 1

	Confidence intervals of transverse on longitudinal		**Confidence intervals of longitudinal on transverse**	
Confidence interval	**2.5%**	**97.5%**	**2.5%**	**97.5%**
Intercept	-3.73	5.43	-0.51	8.31
Slope	0.92	1.04	0.89	1.01

Table 1: The 95% confidence intervals for two linear regression analyses comparing outer wall pore diameter measured from longitudinal and transverse sections.

915 **Table 2**

	Aldan	Byd'yangaya	Churan	Oy- Muran (To-At)	Oy- Muran (At-Bo)	Titirikteekh	Zhurinskiy Mys'
Aldan		0.0301	0.0863	**0.00017**	**0.00376**	**0.00406**	**0.00816**
Byd'yangaya	0.415		0.535	**0.0103**	0.191	0.0974	0.303
Churan	0.486	0.263		0.0633	0.510	0.582	0.414
Oy- Muran (To)	0.661	0.351	0.450		0.290	0.0668	0.115
Oy- Muran (At)	0.525	0.219	0.275	0.225		0.213	0.708
Titirikteekh	0.493	0.217	0.249	0.266	0.204		0.603
Zhurinskiy Mys'	0.500	0.204	0.300	0.282	0.157	0.153	

916 Table 2: Comparing the outer wall pore distributions by locality. The p-values for each pair of
917 localities are shown above the diagonal line of black boxes, with bold text indicating significant
918 results at 95% confidence after the Benjamini-Hochberg procedure. Below the line are the D-
919 values associated with the p-values.

920

921 **Table 3**

	Aldan	Byd'yangaya	Churan	Oy-Muran (To-At)	Oy-Muran (At-Bo)	Titirikteekh	Zhurinskiy Mys'
Median	52.3	62.9	63.6	90.9	75.9	72.2	72.3
Mean	53.0	70.3	85.1	102.4	89.0	79.8	84.9

922 Table 3: Mean and median outer wall pore sizes for the archaeocyaths measured at each locality.
923 To = Tommotian; At = Atdabanian.

924

925 **14. Figure Captions**

926 Figure 1. A: Schematic reconstruction of a double walled archaeocyath showing the major
927 characters discussed in the text. Adapted from a version in (Antcliffe et al. 2014) from the original
928 drawing of (Debrenne et al. 1989). B-F: Archaeocyatha from the Siberian Platform in Russia,
929 Terreneuvian to Cambrian Series 2 in age. B: A thin section of two archaeocyaths, central large
930 specimen is in slightly oblique to longitudinal section, whilst the specimen in the bottom left is in
931 transverse section. C: The archaeocyath *Archaeolynthus polaris* showing multiple modules. D:
932 Two cups of an archaeocyath showing no growth avoidance and which are probably con-specific.
933 E: Two cups of different archaeocyathan individuals showing growth avoidance. F: Close up view
934 of the two-walled structure of an archaeocyath showing the inner and outer walls, the septa, the
935 intervallum space, as well as inner wall pores, outer wall pores and septal pores.
936
937 Figure 2. A: Map showing the locality of the Siberian Platform in Russia, showing the extent of
938 the platform with the three major facies tracts of Terreneuvian to Cambrian Series 2 in age. Stars
939 show the position of the fossil localities on the Lena and Aldan rivers from which the samples used
940 in this study were taken. In general, there is a SW-NE trend of increasing palaeo-water depth, with
941 the archaeocyathan reef acting as a barrier between the shallow restricted marine system to the SW
942 and the deeper marine to the NE. Line X-Y denotes the line of section in part B. B: Schematic
943 reconstruction of the facies relationships of the Siberian Cambrian. C: Schematic of a section along
944 the River Lena, with the Pestrotsvet Formation crosshatched. Colours correspond to the timescale
945 in D. Numbers indicate the position of the localities discussed: 1. Titirikteekh. 2. Churan. 3.
946 Byd'yangaya. 4. Zhurinskiy Mys'. 5. Oy-Muran. Highlighted bars show what age the specimens
947 were drawn from for a particular section. After (Kruse et al. 1995) D: Timescale showing current

948 best estimates for how the Siberian sections correlate with the global stage and series boundaries
949 as recognised by the IGCP (Cambrian), compiled from (Gradstein et al. 2012, Kruse et al. 1995,
950 Landing et al. 2013, Rozanov et al. 2008).
951
952 Figure 3. Representative genera of Archaeocyatha from the Siberian fossil sites around the Lena
953 River. All from the collections in the Muséum National d'Histoire Naturelle in Paris. A and B:
954 *Nochoroicyathus*. C: *Coscinocyathus*. D: *Rotundocyathus*. E: *Erismacoscinus*. F: *Tumuliolynthus*.
955
956 Figure 4. A: Schematic reconstruction of a typical archaeocyath showing the relationship of the
957 major anatomical features to both longitudinal and transverse sections. B: Schematic drawing
958 showing how pores in transverse section could appear smaller than the true diameter, if the section
959 passes through anywhere other than the exact centre of the pore. C: Schematic showing how pores
960 in longitudinal view could appear larger than the true restrictive width, depending on the location
961 of the section.
962
963 Figure 5. A range of features associated with pores and apparent restrictive pore widths. A: the
964 three major pore types: red arrow = outer wall pore; black arrow = septal pore; white arrow = inner
965 wall canal. B: Varying pore sizes seen in slightly oblique section, with pores becoming more
966 elliptical (to sub-polygonal) to the right side of the image. C: Annuli are plate-like features (white
967 arrow) which restrict the pore width, and may add spiny and ornate coverings to the pore. D:
968 Tumuli are sphere-like coverings (red arrow) over pores that have one or more openings to allow
969 transit of particles. E: An example of a broken outer wall, producing a space in the wall much
970 larger than the original pore. F: The irregular growth of archaeocyaths (e.g. if the specimens turns

971 through 90^{o} during growth) means that a single section can intersect the specimen in such a way
972 that transverse, oblique, and longitudinal sections can be seen in a single specimen in thin section.
973
974 Figure 6. Plot showing the correlation between outer wall pore measurements in transverse and
975 longitudinal section (n=257 specimens).
976
977 Figure 7. Box plots of outer wall pore sizes measured separately for locality and section
978 orientation. Any locality name with prefix T are measurements from transverse sections, and those
979 localities with prefix L are measurements from longitudinal sections. The horizontal lines in the
980 boxes represent, in order from top to bottom, the upper quartile, the median, and the lower quartile.
981 Whiskers show the minimum and maximum values excluding outliers. Outliers were defined as
982 being further than 1.5 times the height of the box away from the box and are signified circles. A:
983 Data from all localities studies. B: Enlarged box plots for the two Oy-Muran localities.
984
985 Figure 8: Histogram showing the frequency of archaeocyath specimens with a mean outer wall
986 pore size fall in the given size classes (12 bars, 21µm wide). The global median is 68.8µm and the
987 global mean is 81.5µm. The data is positive skewed with 75% of specimens having pores less
988 than 101µm. The smallest mean restrictive pore size found was 25µm while the largest was 273µm.
989
990 Figure 9: A: Schematic representation of the lining of the mineralised archaeocyath body wall with
991 living cells. These cells would restrict the open pore size. B: Plot to show the percentile effects of
992 the estimated cell thickness on the outer wall pore diameter. The two curves show the maximum
993 possible cell thickness (40µm – lower curve as it has a great effect on open pore diameter) and

minimum possible cell thickness (4µm – upper curve as it has a lesser effect on open pore diameter).

Figure 10: Relationship between the size classification of plankton and the biological function/phylogenetic class of plankton (after Sieburth and Smetacek 1978), note horizontal scale is logarithmic. Phytoplankton consists of photosynthetic single-celled eukaryotic plankton, and all autotrophic and mixotrophic single-celled eukaryotic plankton. Protozooplankton includes all single-celled heterotrophic eukaryotes, such as the ciliates and amoeboids. Metazooplankton includes all metazoan heterotrophic plankton and juvenile planktonic metazoans. The purple shading indicates the density of the data of archaeocyath mean pore sizes. The red line indicates the theoretical maximum length of plankton that could be consumed by the largest restrictive pores found in this study. Based on a typical 3:1 length to width ratio for copepods (Fernandez Araoz 1991) and micro-current alignment of non-spherical prey items (Visser and Jonsson 2000). For a maximum prey body size of therefore 3 x 269µm = 807µm. Rather than simply being capable of eating bacterioplankton in the picoplankton range, even the smallest-pored archaeocyath would have been able to consume the nanoplankton range of the single-celled eukaryotic plankton groups, with several of the archaeocyaths being able to carnivorously consume micro-metazoans.

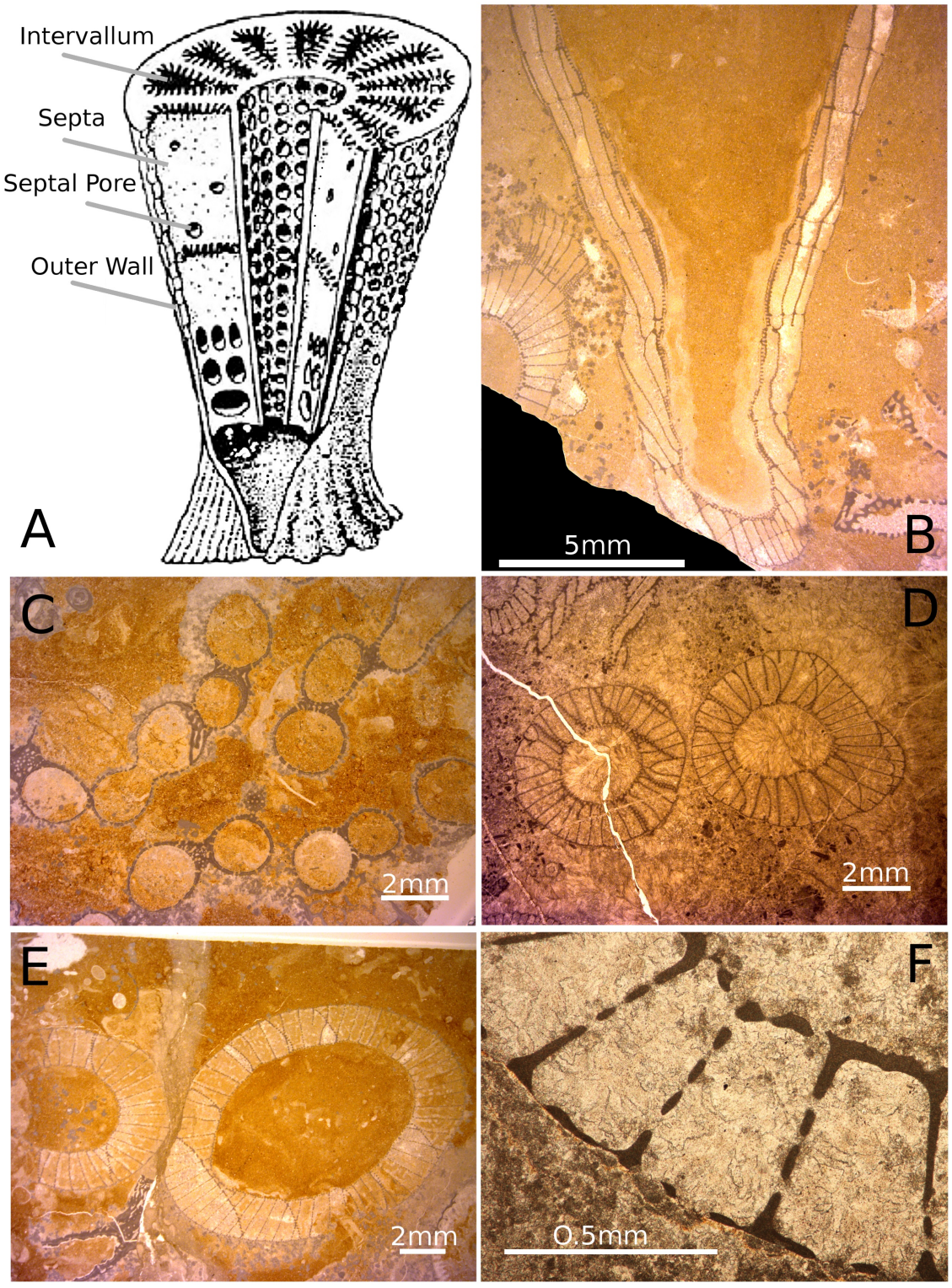
Intervallum
Septa
Septal Pore
Outer Wall
A
5mm
B
C
2mm
D
2mm
E
2mm
F
0.5mm

Figure 1

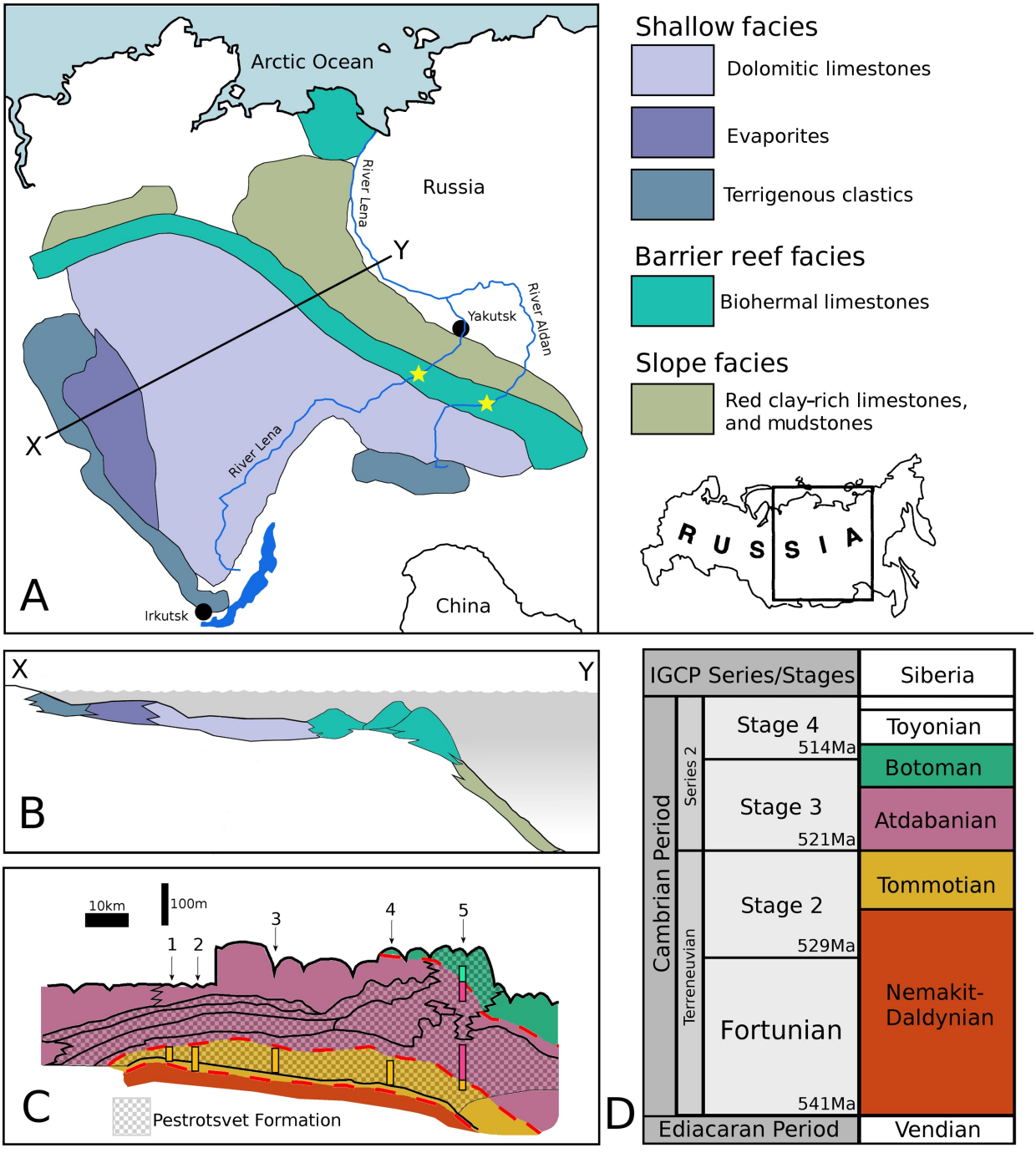

1016

1017 Figure 2

1018

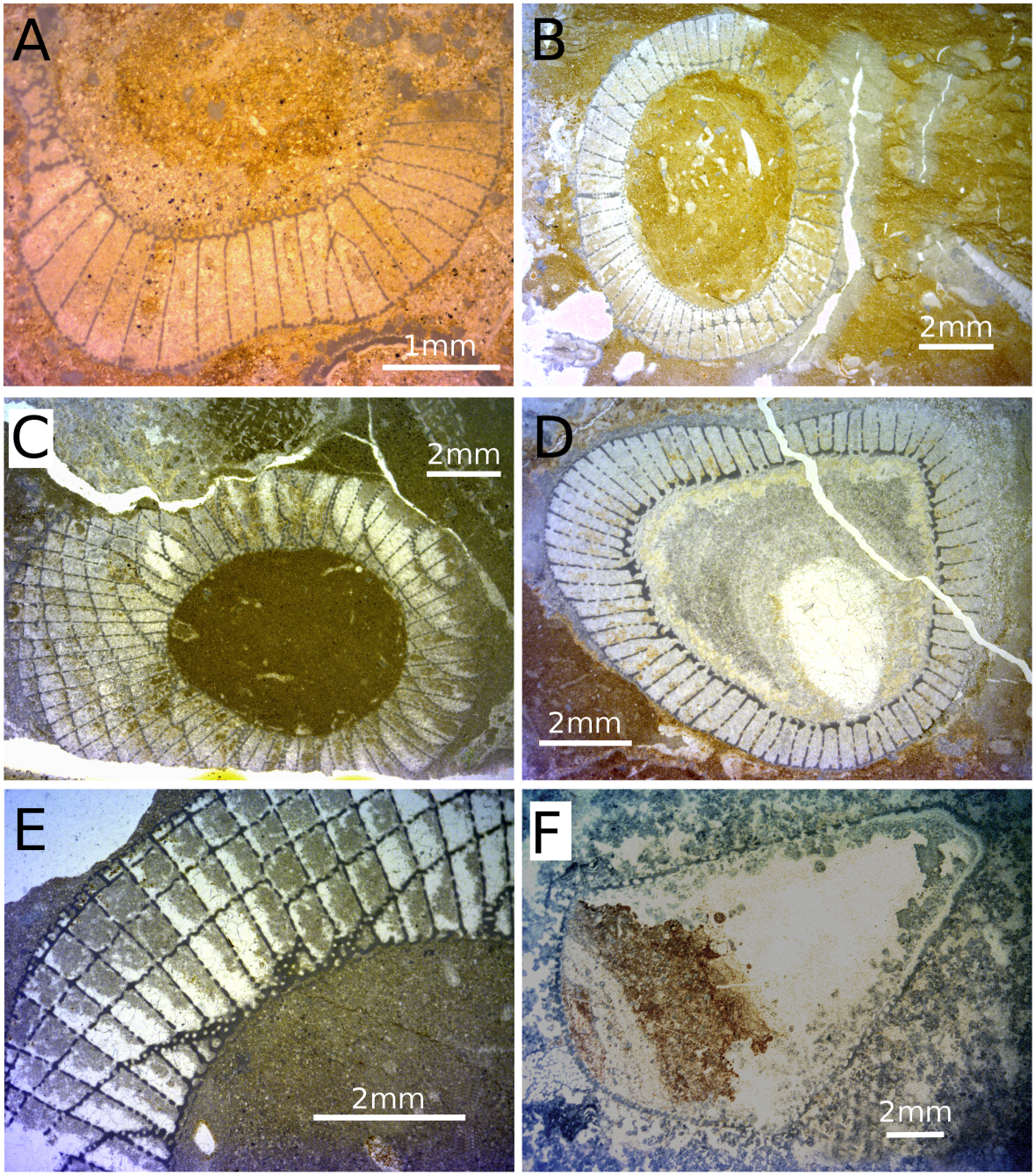

1019

1020 Figure 3

1021

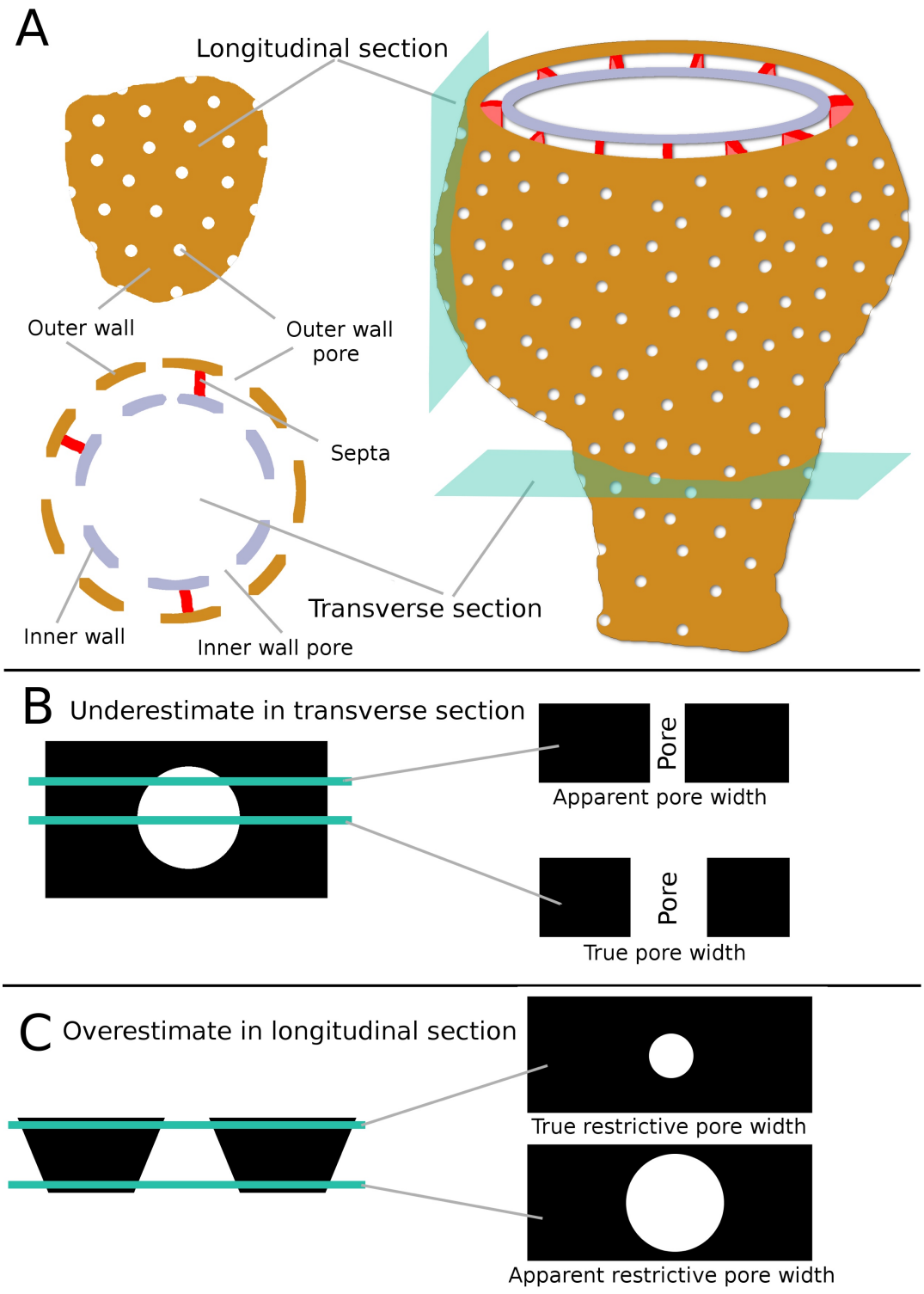

1022

1023 Figure 4

1024

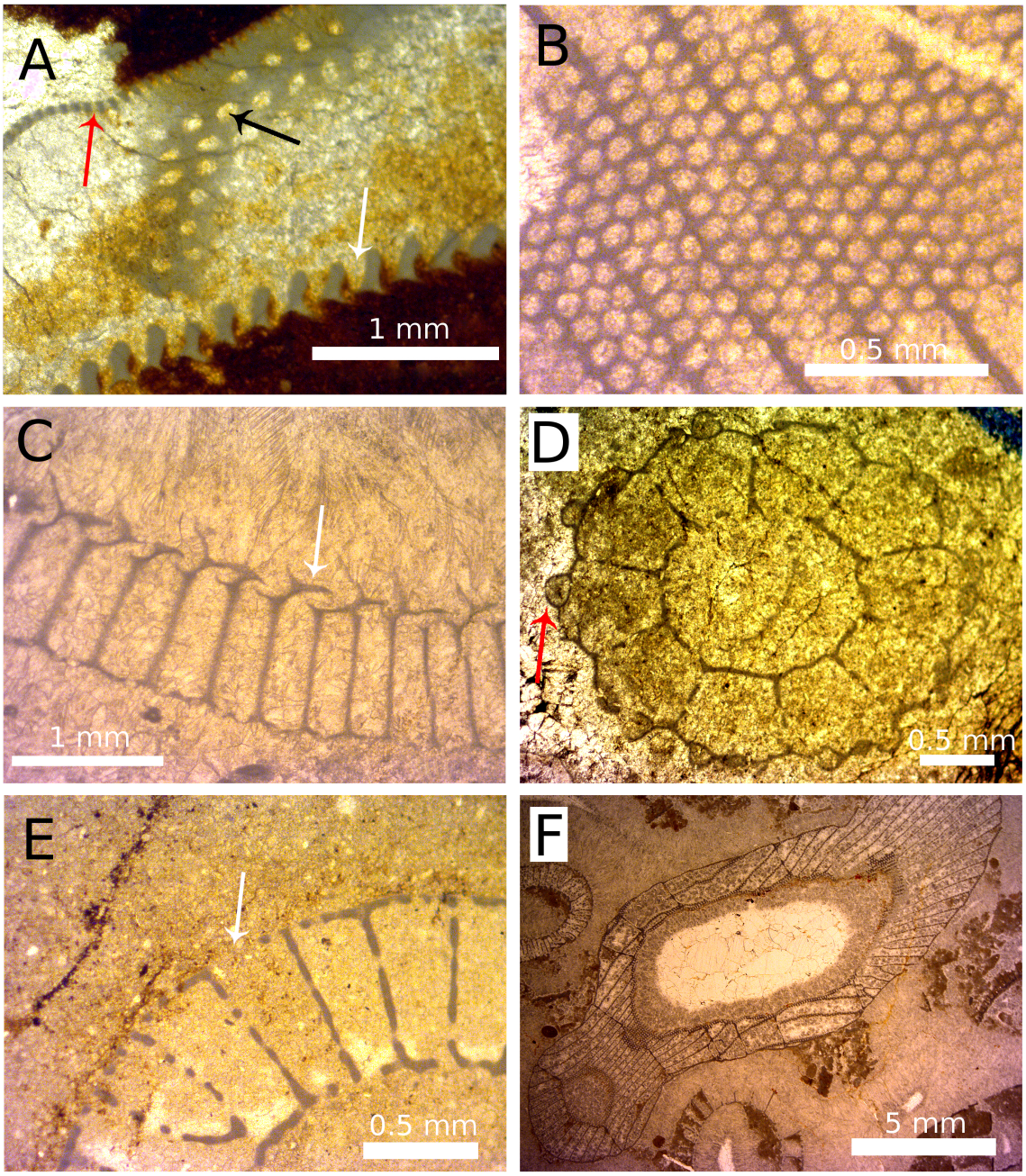

Figure 5

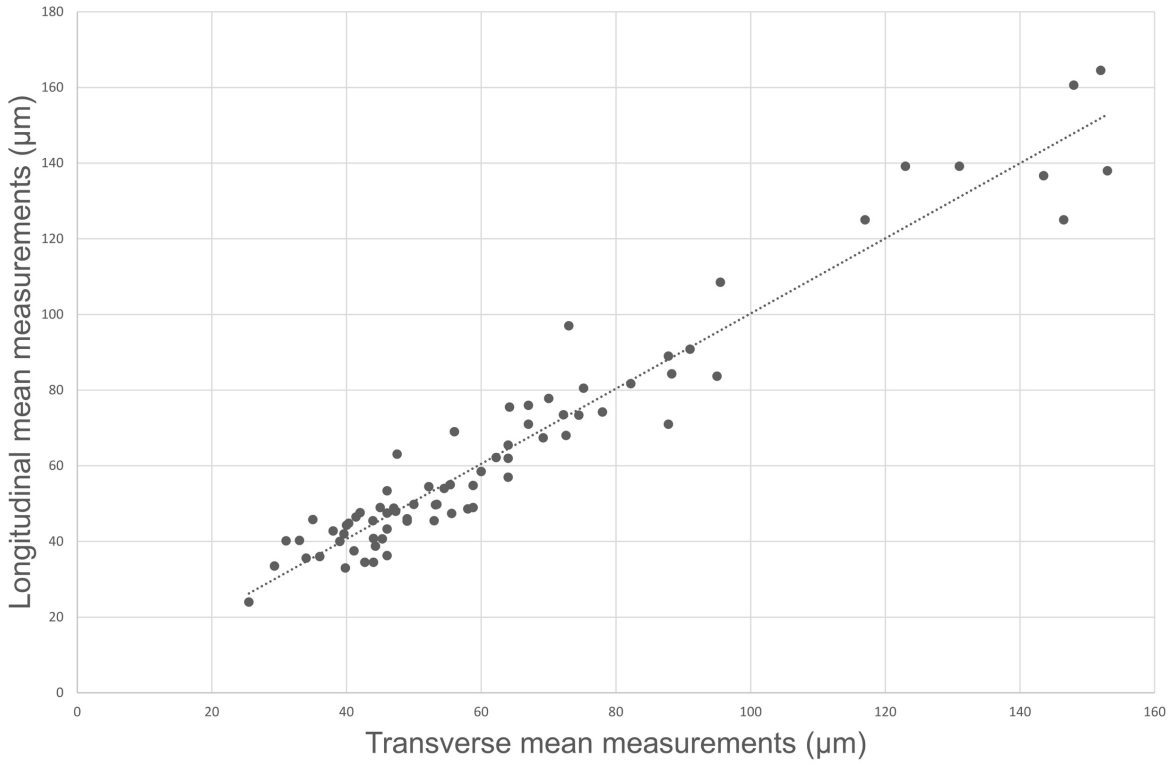

1028

1029 Figure 6

1030

1031

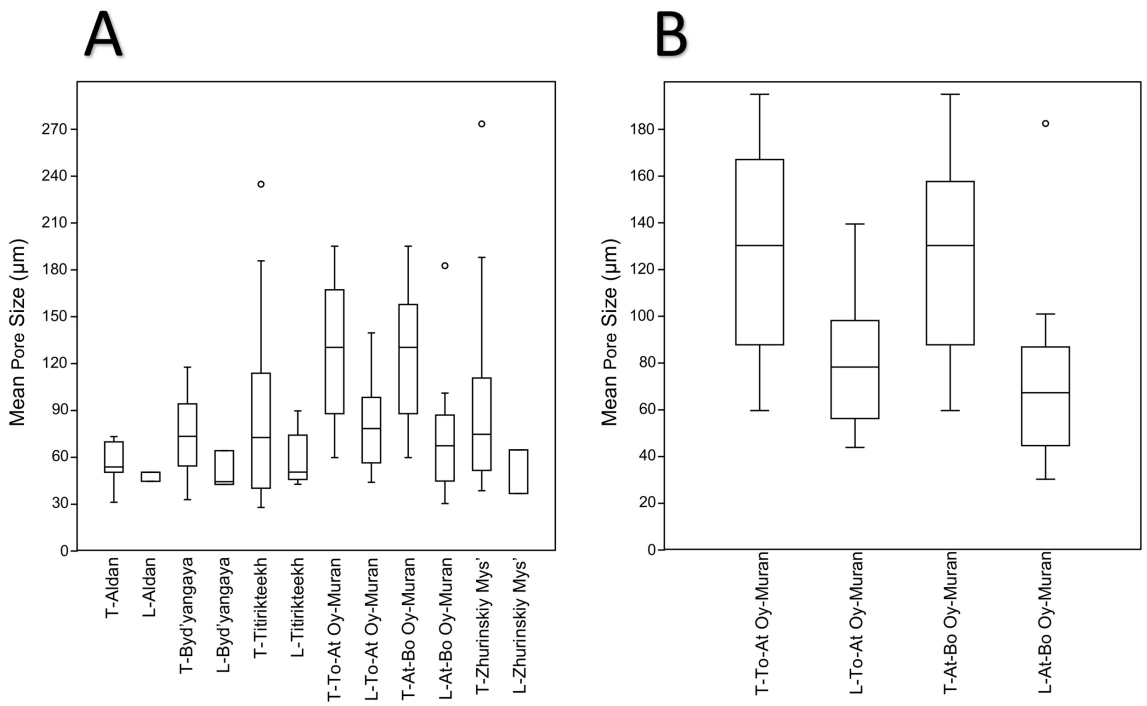

1032

1033 Figure 7

1034

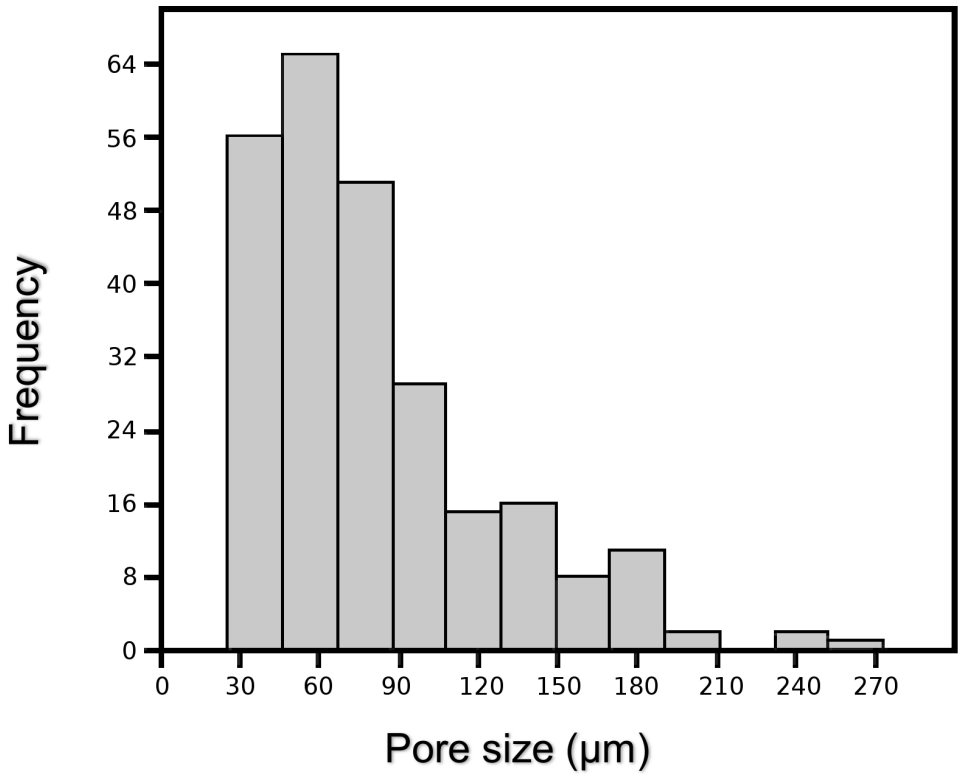
Frequency
64
56
48
40
32
24
16
8
0
0
30
60
90
120
150
180
210
240
270
Pore size (μm)

Figure 8

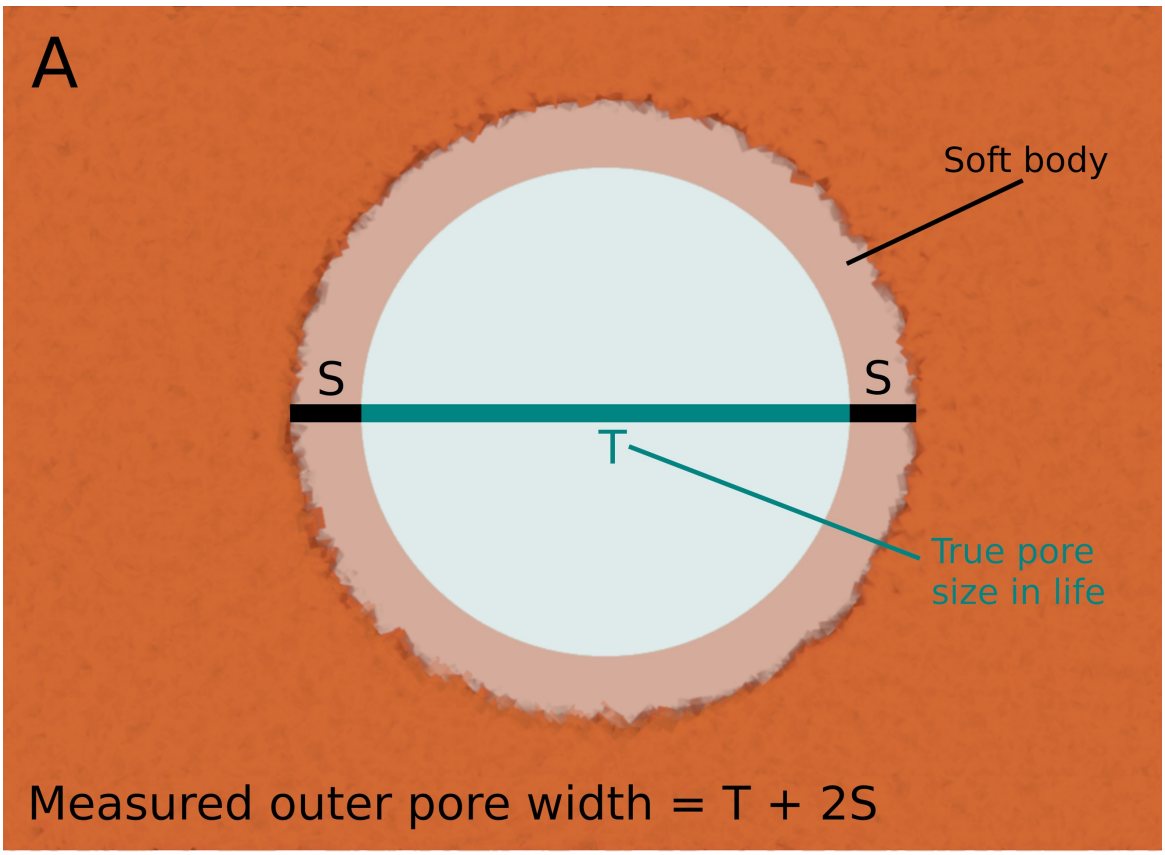

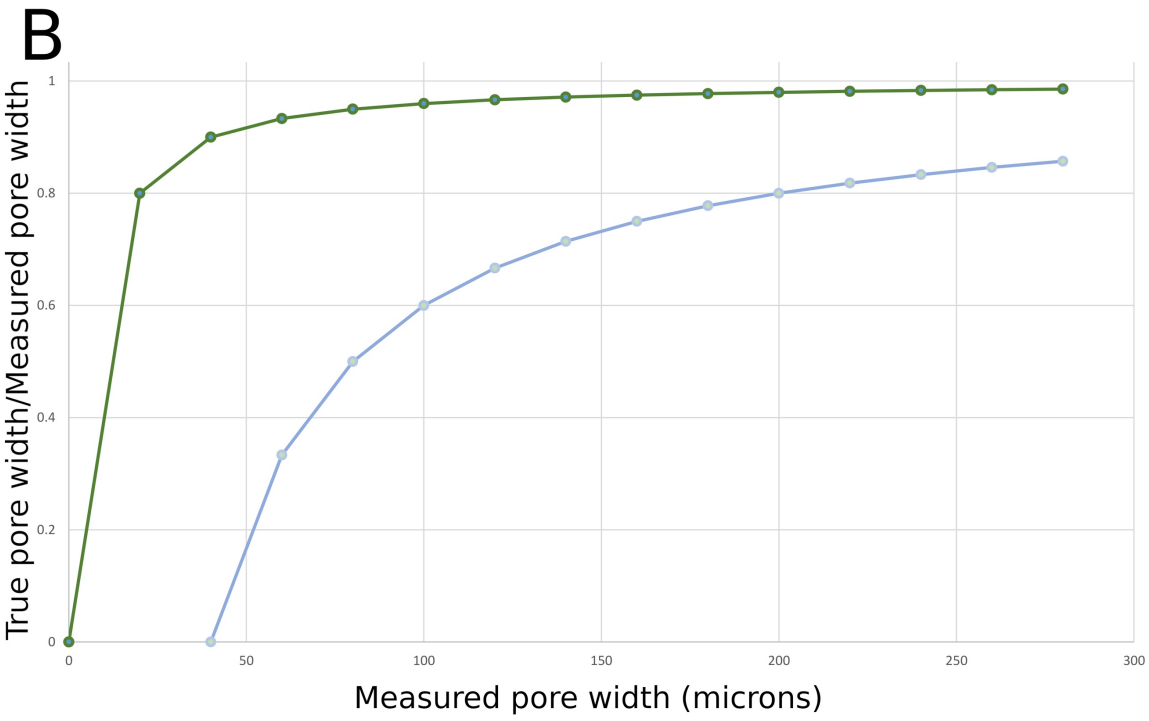

1040

1041 Figure 9

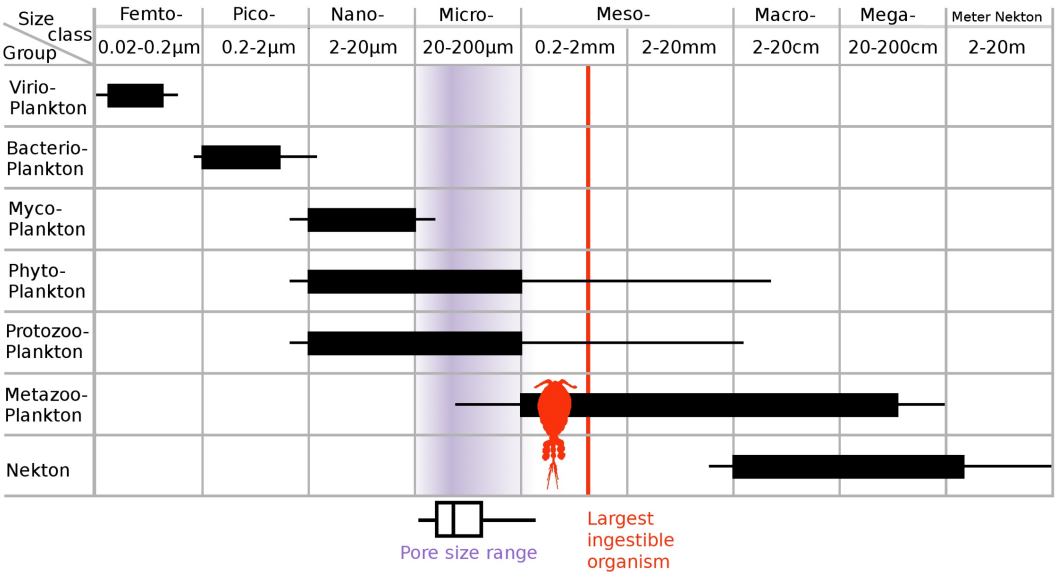

1042

1043 Figure 10